

VIRTUAL GAP ANALYSIS PROCEDURES FOR MULTI-CRITERIA DECISION-MAKING AND EFFICIENCY ANALYSIS PROBLEMS

FUH-HWA FRANKLIN LIU *

*Professor Emeritus, Department of Industrial Engineering and Management,
National Yang Ming Chiao Tung University, Taiwan 300, Republic of China*

SU-CHUAN SHIH †

*Associate Professor, Department of Business Administration,
Providence University, Taiwan 433, Republic of China*

Received 7 June 2024

Revised 22 January 2025

Accepted 24 June 2025

Existing multi-criteria decision-making (MCDM) methods often face challenges when evaluating a large number of alternatives, leading to skewed results in selecting the optimal choice. Similarly, conventional efficiency analysis (EA) methods, such as Data Envelopment Analysis (DEA) and Stochastic Frontier Analysis (SFA), often yield incomplete solutions due to their reliance on theoretical assumptions. To address these limitations, we propose a novel EA method that integrates Virtual Gap Analysis (VGA) models to evaluate the performance of each decision-making unit (DMU) in relation to others based on best practices. Unlike DEA and SFA, our VGA models are linear programming-based, assumption-free, and capable of delivering robust and reliable solutions. The proposed method enables each DMU to identify achievable benchmarks for inputs and outputs. Based on the estimated virtual gaps, DMUs are classified as inefficient (with scores below one) or efficient (with scores of one or higher). Additionally, our new MCDM method incorporates existing MCDM techniques to analyze the few identified efficient DMUs, significantly reducing the effort required to select the best DMU.

Keywords: Decision Support System; Multiple Criteria Decision Making; Efficiency Analysis.

MSC: 90B50; 90C29; 90C08; 91A80; 91B06.

*corresponding author; fliu@nycu.edu.tw

†scshih@gm.pu.edu.tw

1. Research Background and Objectives

1.1. The Traditional EA and MCDM Methods

Table 1 presents a numerical example involving six firms—K, A, B, D, G, and H—that consume resources X_1 and X_2 to produce products Y_1 and Y_2 in varying amounts. The resources and products have different measurement units, and for some firms, market prices per unit of the resources and products are unavailable. Interactions between the resources and products are disregarded. The observed dataset consists exclusively of positive, continuous real numbers.

The observed dataset can be described as a discrete multi-criteria assessments (MCA) problem with n alternatives (firms) evaluated based on m minimization criteria (resources) and s maximization criteria (products). Each alternative has an observed score for each criterion, measured using a commensurable scale unit. The MCA method employs a mathematical algorithm to determine the weights of the criteria. The decision-maker ranks the alternatives according to their total weighted scores and selects the best one.

A typical MCA problem aims to evaluate each object decision-making unit (firm), denoted as DMU_o , against n DMUs (firms) using m inputs (resources) and s outputs (products). Each EA approach employs a mathematical framework to assess the *relative efficiency* of DMU_o , pinpointing the necessary changes in inputs and outputs to attain a relative efficiency score of 1. Each DMU within the collection of DMUs is evaluated in turn as DMU_o .

While MCA problems rely on the observed dataset, their objectives differ. In this paper, the terms alternatives, minimization criteria, and maximization criteria are used interchangeably with DMUs, inputs, and outputs.

Table 1. Numerical example of the MCA problems.

Criteria		Alternative-j (or DMU_j)						Decision variables	
Minimization vs. Maximization		K	A	B	D	G	H	Adjustment ratios	Virtual Unit prices
Input- X_1	x_{1j} (ton)	1.6	2.3	1	1.9	1.8	2.5	q_{1o}	v_{1o} (\$/ton)
Input- X_2	x_{2j} (hr)	145	120	29	281	250	100	q_{2o}	v_{2o} (\$/hr)
Output- Y_1	y_{1j} (m^3)	1036	1327	567	2446	1794	1000	p_{1o}	u_{1o} (\$/ m^3)
Output- Y_2	y_{2j} (%)	49	97	89	97	57	70	p_{2o}	u_{2o} (\$/%)
							Decision variables	Systematic parameters	
Variable Intensities		π_{oK}	π_{oA}	π_{oB}	π_{oD}	π_{oG}	π_{oH}	$\kappa_o^1, \kappa_o^z, \kappa_o^2, \tau_o^*(\$)$	

Since the 1960s, numerous multiple criteria decision-making (MCDM) methods have provided systematic frameworks for addressing complex decision-making problems across various fields ¹. Sahoo and Goswami ¹ conducted a comprehen-

sive review of MCDM methods, highlighting their advancements, applications, and potential future directions. Their study explored widely used MCDM methods, including AHP, TOPSIS, ELECTRE, PROMETHEE, DEA, MUAT, GRA, ANP, Fuzzy TOPSIS, and MOO. They noted that these methods are often constrained by subjective judgments and susceptible to individual biases. In our research, we argue that MCDM methods should limit the number of alternatives considered to ensure reliable and meaningful results. Decision-makers require a systematic approach to reduce the number of alternatives, mainly when subjective judgments play a critical role in the decision-making process.

In specific scenarios, different MCDM methods yield significantly divergent rankings. Amor et al.² analyzed 1,921 MCDM-related documents in English, published between 1990 and 2021. From this dataset, they selected 659 articles and 16 reviews as their final sample. They imported the corresponding BIB files containing complete records and cited references to perform bibliometric analysis using the bibliometrix tool. The statistical data were employed to map academic research on discrete multi-criteria decision analysis methods and their applications in sorting, classification, and clustering. Their study focused on nine widely used MCDM methods for practical applications. Regardless of the mapping approach, their findings revealed that existing MCDM methods often produce varying results, which can be a source of debate.

Data Envelopment Analysis (DEA)^{3 4} is one of the major MCA methods. Introduced in 1978, DEA employs linear programming⁵ to estimate the adjustments and weights of the inputs and outputs of each decision-making unit (DMU), denoted as DMU_o . DEA's significant contributions have spurred extensive research in the field of MCA. Over the past 50 years, hundreds of textbooks and thousands of journal articles related to DEA have been published⁶. Sickles and Zelenyuk⁷ provided a comprehensive review of MCA methods and the underlying assumptions of DEA theory. DEA models measure DMU_o 's relative efficiencies under the conditions of constant returns-to-scale (CRS) and variable returns-to-scale (VRS). The Additive Models have yielded incomplete solutions⁸. The drawbacks of the original DEA models have been comprehensively discussed^{9 10 11 12 13 14}.

The statistic-based Stochastic Frontier Analysis (SFA)¹⁵ is another foundational method in efficiency analysis (EA). SFA assumes that the estimation of the *average production frontier* consists of two independent randomness components. One error term represents *technical efficiency*, which is assumed to be negative due to DMU_o 's inability to reach the production frontier. The other error term accounts for unobservable and measurement difficulties. The deviation of DMU_o from the mean efficiency can be calculated to evaluate the extent of its inefficiency. The average production frontier function is estimated by assuming that the errors follow a half-normal distribution and applying maximum likelihood estimation techniques. Madaleno and Moutinho¹⁶ discussed comparisons between DEA and SFA, noting that the reliability of the SFA model diminishes when the dataset does not satisfy its underlying assumptions. Over the past 50 years, thousands of articles and

numerous textbooks have been published on SFA.

1.2. Research Objectives

This paper introduces a novel perspective and addresses the key limitations of traditional EA and MCDM methods. Figure 1 presents the flowchart of our new EA method, the *Virtual Gap Analysis (VGA) procedure* based on best practices, abbreviated as b-VGA-EA. In this approach, each decision-making unit (DMU_o) evaluates itself against other DMUs to estimate the virtual gap. Figure 2 illustrates

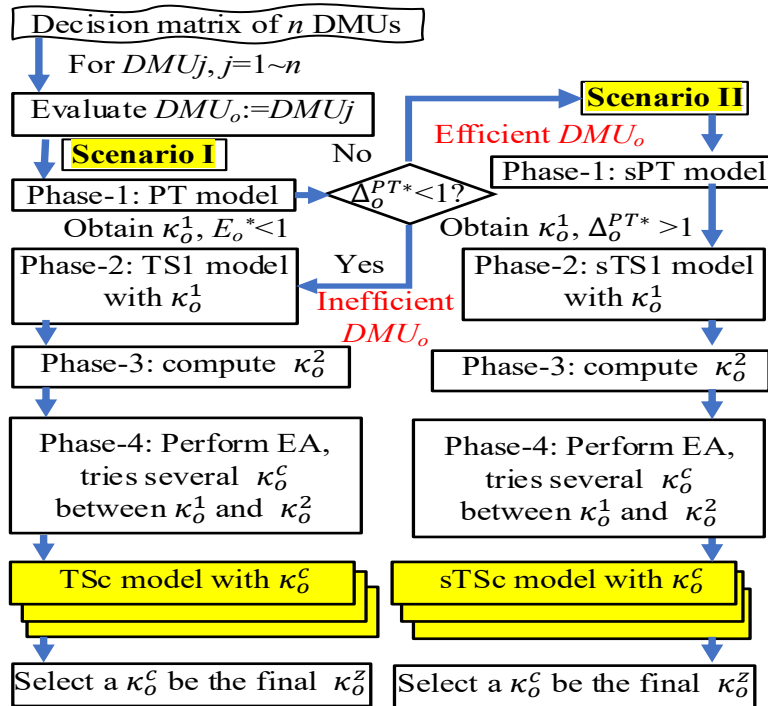


Fig. 1. The x b-VGA-EA method to assess DMUs.

our new MCA method, termed b-VGA, which integrates the b-VGA method to reduce the number of DMUs. This reduction allows for the efficient application of existing MCDM techniques to identify the best-performing DMU.

Finally, this paper explores EA and MCDM methods from the perspective of worst practices, where inputs and outputs are inverted. Using the MCDM method, the least efficient DMU can be effectively identified.

1.2.1. Our EA method, b-VGA-EA method

In Figure 1, Scenario I comprises four phases using the *best-practice pure technical efficiency* (PT) and *best-practice technical and scalar choice efficiency* (bTSc) VGA models. Scenario II includes the *super-pure technical efficiency* (sPT) and *super-technical and scalar choice efficiency* (sTSc) VGA models. The four linear VGA models are detailed in Sections 2 and 3. A basic understanding of linear programming⁵ is required to comprehend the b-VGA-EA method fully.

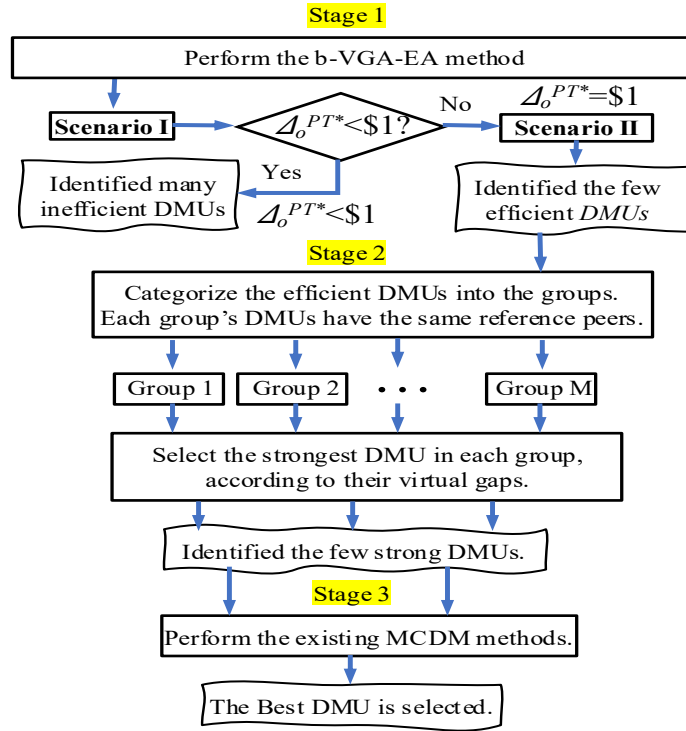


Fig. 2. The b-VGA-MCDM method to select the best alternative.

The four VGA models utilize decision variables $(q_{1o}, q_{2o}, p_{1o}, p_{2o})$ and $(v_{1o}, v_{2o}, u_{1o}, u_{2o})$ to represent the *adjustment ratios* and *virtual unit prices* of (X_1, X_2, Y_1, Y_2) , respectively. The decision variables $\pi_{oK}, \pi_{oA}, \dots,$ and π_{oH} denote the *intensities* of the six DMUs in evaluating DMU_o . The parameter *unified goal price*, $\tau_o^*(\$)$, is systematically determined in two steps and serves as the common lower bound for the variable *total virtual prices* of $X_1, X_2, Y_1,$ and Y_2 . The estimated optimal value of a decision variable in each VGA model is denoted with the superscript '★'. The vector form of the estimated values are $(q_o^*, p_o^*), (v_o^*, u_o^*),$ and π_o^* .

In the bTSc and sTSc models, the additional sum of the intensities condition (SIC) requires the summation of variable intensities to equal a chosen scalar κ_o^c . The SIC corresponds to the dual variable w_o . Each model produces the systematic parameters κ_o^1 and κ_o^2 . DMU_o selects κ_o^z , a value between κ_o^1 and κ_o^2 , to determine achievable adjustment ratios (q_o^* , p_o^*) for optimizing its performance.

In each model, a positive $\pi_{o_j}^* > 0$ indicates that DMU_j is one of the *reference peers* of DMU_o . Each input (or output) DMU_o is adjusted to the sum of the inputs (or outputs) of the reference peers, weighted by their respective intensities.

Scenario I estimates the reduction of inputs (q_o^*) and the expansion of outputs (p_o^*). The PT model calculates the virtual gap of DMU_o , denoted as Δ_o^{PT*} , which represents the excess of *virtual input* ($x_o v_o^*$) over *virtual output* ($y_o u_o^*$). If $\Delta_o^{PT*} < \$1$, DMU_o is considered inefficient. In this scenario, DMU_o proceeds to choose κ_o^z in Phase-4 to achieve feasible values of q_o^* and p_o^* . The resulting virtual gap is $\$0 \leq \Delta_o^{bTSz*} \leq \1 , which is equal to the minimal value of $x_o v_o^* - y_o u_o^* + \kappa_o^{bTSz} \times w_o^*$. This reduction of the virtual gap to \$0 indicates that there is room for improvement in inputs and outputs by adjusting the ratios q_o^* and p_o^* .

Conversely, if $\Delta_o^{PT*} = \$1$, DMU_o is deemed efficient. In Scenario II, DMU_o proceeds to choose κ_o^z in Phase-4 to determine feasible q_o^* and p_o^* values. The virtual gap in this case is $\$1 \leq \Delta_o^{sTSz*}$, which is equal to the minimal value of $-x_o v_o^* + y_o u_o^* + \kappa_o^{sTSz} \times w_o^*$. Reducing this virtual gap to \$1 reflects that DMU_o possesses buffers for deterioration in inputs and outputs, which can be achieved by adjusting ratios q_o^* and p_o^* through expansion and reduction, respectively.

Table 2 summarizes the solutions in assessing the inefficient DMU_K . In column TS3-II, the optimal solutions of the decision variables for the TS3 VGA model can be found. DMU_B and DMU_D are the reference peers of DMU_K , with intensities of 0.383 and 0.335, respectively.

Figures 3 and 4 present the results of the assessments for the PT, TS1, and TS2 models, helping users better understand the b-VGA-EA method. The relationship between relative, technical, and scale efficiencies can be visualized in the 2D graphical representations. Similarly, the EA reports for the efficient DMU_B and DMU_D are shown on the right-hand side of Table 2 and in the entire Table 3.

Table 3 summarizes the b-VGA-EA method reports in assessing the efficient DMU_B and DMU_D . Figures 5 and 6 display 2D graphical representations of the assessments by the sTS1 and sTS2 models. These figures help visualize the relationship between relative, technical, and scale efficiencies. The technical and scale efficiencies have not been numerically computed at this stage.

DMU_B 's relative efficiency score in the sTSz evaluation is 2.4479. According to the adjustment ratios DMU_B in column sTSz-II, the ranking of strengths is as follows: Y_2 , X_2 , Y_1 , and X_1 , with X_1 being the weakest. These rankings differ from those observed in the sTS1 and sTS2 evaluations. The results of this numerical example demonstrate the depth of the EA method and its ability to provide insightful assessments.

1.2.2. *Our MCDM method, b-VGA-MCDM method*

Figure 2 displays the b-VGA-MCDM method. In the first stage, the b-VGA-EA method is applied to identify the efficient DMUs, typically resulting in only a few efficient DMUs. These efficient DMUs, sharing the same reference peers, are categorized into groups in the second stage. Within each group, the efficient DMU with the highest virtual gap outperforms the others, and those with lower super-efficiency are excluded from consideration in the third stage. In the third stage, decision-makers can efficiently use existing MCDM methods to select the best DMU from the remaining candidates. They may also introduce several uncertain or qualitative criteria, as subjective judgment is often necessary. In some cases, when the number of candidates is minimal, decision-makers may not need to apply any existing MCDM methods.

In our numerical example, DMU_B and DMU_D have two different sets of reference peers. These DMUs are compared in the third stage. Decision-makers may assess the persistence capability of DMU_B and DMU_D with respect to their inputs and outputs. This study provides decision-makers with valuable insights and enables informed decision-making in dynamic selection environments.

1.3. *Early VGA Developments*

Hwang¹⁷ contributed to establishing CRS and VRS VGA models, where the former excludes and includes the SIC, equating to 1. However, issues arose concerning the virtual goal price DMU_o and the relationship between these models. The virtual goal price was subjectively assigned. Past research, including works by Liu and Liu¹⁸¹⁹, applied the CRS VGA model in two-phase production systems. The authors have provided consultation on unpublished theses that utilized these models. Specifically, Lin²⁰ and Li²¹ applied the PT model in their respective thesis studies.

1.4. *Paper Organization*

This paper is organized as follows: Section 2 introduces the PT and bTSc VGA models for assessing efficiency. Section 3 discusses the sPT and sTSc VGA models for determining super-efficiency. Section 4 describes the four-phase b-VGA-EA method. Section 5 presents a numerical example to illustrate the two VGA scenarios. Finally, Section 6 concludes the paper and discusses the findings. Readers familiar with DEA may be interested in comparing DEA and VGA. To address this, we have included 26 footnotes to highlight how DEA models have inspired VGA models and to explain why DEA models cannot achieve certain aspects of efficiency analysis that VGA models can.

2. **Scenario-I: Evaluating DMUs' Inefficiencies**

Scenario-I assesses the inefficiencies of DMUs by the PT and bTSc VGA models in a four-phase procedure.

2.1. Notations

The following notations are used in VGA models. The set J , I , and R , respectively, denotes the set of n DMUs, m inputs, and s outputs. The *decision matrix*, denoted as (X, Y) , consists of column vectors (x_j, y_j) , in which the elements (x_{ij}, y_{rj}) represent positive *observed volume* of each $Input_i$ (X_i) and $Output_r$ (Y_r) of each DMU_j .ⁱ

The decision variables (q_{io}, p_{ro}) ⁱⁱ and (v_{io}, u_{ro}) ⁱⁱⁱ denote the dimensionless *adjustment ratios* and *virtual unit prices* (\$) of (X_i, Y_r) , while their vectors are (q_o, p_o) and (v_o, u_o) . π_{jo} denotes the variable *intensity* of DMU_j in evaluating DMU_o , and π_o is the vector form.

We developed a *two-step process* to determine a systematic *unified goal price* τ_o , measured in the virtual currency \$.^{iv} The superscripts # and * indicate the optimal solutions for a decision variable in each VGA model, respectively, for Step I and Step II.

The symbol w_o is the *scalar unit price* (\$) corresponding to the SIC.^v κ_o^c is the SIC scalar in the bTSc and sTSc VGA models. ω_o^c is the *virtual scalar price* (\$) of the SIC model $\kappa_o^c \times w_o$.

2.2. Pure Technical Efficiency (PT) model

The dual program of the PT model.

$$\Delta_o^{PT*}(\$) = \max_{q_o, p_o, \pi} \sum_{\forall i \in I} q_{io} \tau_o(\$) + \sum_{\forall r \in R} p_{ro} \tau_o(\$), (\forall o \in J); \quad (1)$$

ⁱ Cooper et al.⁴ introduced Equations (3.1) and (4.1) to represent the production possibility set (PPS) derived from the observed data of DMUs. The PPS without the convexity condition $e\lambda = 1$ is referred to as the constant returns-to-scale (CRS) PPS, while the PPS with the convexity condition is known as the variable returns-to-scale (VRS) PPS. Each PPS is characterized by an efficiency frontier that envelops each DMU_o at (x_o, y_o) .

$P^{CRS} = \{(x_o, y_o) | x_o \leq X\lambda, y_o \geq Y\lambda, \lambda \geq 0.\}$
 $P^{VRS} = \{(x_o, y_o) | x_o \leq X\lambda, y_o \geq Y\lambda, (e\lambda = 1,)\lambda \geq 0.\}$

Cooper et al.⁴ presented the envelopment and multiplier programs of the Additive Model, given by Eqs. (4.34)–(4.38) and Eqs. (4.39)–(4.43), to estimate the vector of variable intensities λ . The model applies the production theory of neoclassical economics to evaluate DMU_o can be effectively characterized by the PPS. The PPS is defined by four key properties⁴.

Chapters 1 and 2 in Sickles and Zelenyuk⁷ provide twenty graphical illustrations of PPS in two dimensions, offering theoretical insights into CRS and VRS DEA models. However, a graphical representation of the efficiency frontier for PPS involving multiple inputs and outputs has yet to be developed.

ⁱⁱ Instead, DEA models used the slacks (s_{io}^x, s_{ro}^y) as decision variables, which have various measurement units.

ⁱⁱⁱ DEA models defined (v_{io}, u_{ro}) as dimensionless weights.

^{iv} Instead, each DEA model developer defined the coefficient b_i^x and b_r^y be the the lower bound of weight v_{io} and u_{ro} . The coefficients are called *artificial goal weights*.

^v In the Additive Model, the symbol σ_o is dimensionless and corresponds to the convexity condition, $\sum_{\forall j \in J} \lambda_{oj} = 1$.

$$s.t. \sum_{\forall j \in J} x_{ij} \pi_{jo} + q_{io} x_{io} = x_{io}, \forall i \in I; \quad (2)$$

$$- \sum_{\forall j \in J} y_{rj} \pi_{jo} + p_{ro} y_{ro} = -y_{ro}, \forall r \in R; \quad (3)$$

$$\pi_o, q_o, p_o \geq 0. \quad (4)$$

Eq. (2) and Eq. (3) correspond to the primal program's variable unit prices, v_{io} and u_{ro} . Eq. (1) measures the *maximum total adjustment price* (TAP) of DMU_o .

The primal program of the PT model aims to measure the minimum *total virtual gap* (TVG):^{vi}

^{vii} ^{viii} The *virtual gap condition* Eq. (6) limits each DMU_j to a total virtual gap, the excess of *virtual input* and *virtual output*, to a minimum of \$0. Eq. (7) and Eq. (8) restrict the *virtual price* of X_i and Y_r to a unified lower bound *unified goal price* τ_o .

Eq. (6), Eq. (7), and Eq. (8) correlate with the dual program's decision variable π_{jo} , q_{io} , and p_{ro} , respectively. In Step I and Step II, substitute τ_o by $\tau_o^\# = \$1$ and $\tau_o^* = \$\bar{l}$, respectively.

$$\Delta_o^{PT^*}(\$) = \min_{v_o, u_o} \sum_{\forall i \in I} v_{io} x_{io} - \sum_{\forall r \in R} u_{ro} y_{ro}, (\forall o \in J); \quad (5)$$

^{vi} Halická and Trnovská⁸ extensively reviewed DEA models and proposed a unified model to encompass various DEA approaches that address the Additive Model under VRS conditions, see footnote i. Without the four parentheses terms, it becomes the CRS Additive Model.

The envelopment program:

$$F_o^* = \max_{\pi_o, s_o^x, s_o^y} \sum_{\forall i \in I} s_{io}^x b_i^x + \sum_{\forall r \in R} s_{ro}^y b_r^y, \forall o \in J; \text{ s.t. } \sum_{\forall j \in J} x_{ij} \lambda_{oj} + s_{io}^x = x_{io}, \forall i \in I; - \sum_{\forall j \in J} y_{rj} \lambda_{oj} + s_{ro}^y = -y_{ro}, \forall r \in R; (\sum_{\forall j \in J} \lambda_{oj} = 1); \lambda_{oj}, \forall j \in J; s_{io}^x, \forall i \in I; s_{ro}^y, \forall r \in R \geq 0.$$

The multiplier program:

$$f_o^* = \min_{v_o, u_o, \sigma_o} \sum_{\forall i \in I} v_{io} x_{io} - \sum_{\forall r \in R} u_{ro} y_{ro} (+\sigma_o), \forall o \in J; \text{ s.t. } \sum_{\forall i \in I} v_{io} x_{ij} - \sum_{\forall r \in R} u_{ro} y_{rj} (+\sigma_o) \geq 0, \forall j \in J; v_{io} \geq b_i^x, \forall i \in I; u_{ro} \geq b_r^y, \forall r \in R; v_{io}, \forall i \in I; u_{ro}, \forall r \in R, (\sigma_o) \text{ free.}$$

^{vii} See footnote vi. The envelopment program of the DEA Additive Models evaluates dimensionless relative inefficiency as the total dimensionless slacks of inputs and outputs. However, a critical flaw lies in the fact that these slacks, s_{io}^x and s_{ro}^y , actually possess distinct measurement units, contradicting the assumption of dimensional homogeneity.

^{viii} Several DEA axioms fail to satisfy the fundamental conditions necessary for formulating linear programs. The decision variables, constraints, and objective functions of VGA models differ significantly from those of DEA Additive Models. Consequently, it is essential to abandon traditional DEA theory and instead formulate VGA models with both primal and dual programs to ensure their verification through duality principles. Unlike DEA models, VGA models define decision variables and coefficients in their actual measurement units, maintaining consistency with real-world data.

$$s.t. \sum_{\forall i \in I} v_{io} x_{ij} - \sum_{\forall r \in R} u_{ro} y_{rj} \geq 0(\$), \forall j \in J; \quad (6)$$

$$x_{io} v_{io} \geq \tau_o(\$), \forall i \in I; \quad (7)$$

$$y_{ro} u_{ro} \geq \tau_o(\$), \forall r \in R; \quad (8)$$

$$v_o, u_o \text{ free}. \quad (9)$$

The optimal solutions of Eq. (1) in Step I and Step II are depicted in Eq. (10). Eq. (11) expresses the multiple inputs and outputs of each DMU_j in Step I and Step II are aggregated into the pairs of $(\alpha_j^\#, \beta_j^\#)$ and (α_j^*, β_j^*) . In Step I, $\Delta_o^{PT\#}$ it may exceed that \$1.

$$\begin{aligned} \$0 \leq \Delta_o^{PT\#} &= \sum_{\forall i \in I} q_{io}^\# \times \$1 + \sum_{\forall r \in R} p_{ro}^\# \times \$1; \\ \$0 \leq \Delta_o^{PT^*} &= \sum_{\forall i \in I} q_{io}^* \tau_o^* + \sum_{\forall r \in R} p_{ro}^* \tau_o^* \leq \$1. \end{aligned} \quad (10)$$

$$\$0 \leq (TVG) = (vInput) - (vOutput);$$

$$\$0 \leq \Delta_j^{PT\#} = v_o^\# x_j - u_o^\# y_j = \alpha_j^\# - \beta_j^\#; \quad (11)$$

$$\$0 \leq \Delta_j^{PT^*} = v_o^* x_j - u_o^* y_j = \alpha_j^* - \beta_j^* \leq \$1.$$

DMU-o determines its unified goal price τ_o^* to ensure $\Delta_o^{PT^*}$ and $\Delta_o^{PT\#}$ in Step II are within the range of $(\$0, \$1)$. The relationship $\tau_o^\# : \tau_o^* = 1 : \bar{t} = \Delta_o^{PT\#} : \Delta_o^{PT^*}$ could be derived from the *relation equation* $\bar{t}(\alpha_o^\# - \beta_o^\#) = 1(\alpha_o^* - \beta_o^*)$. Use Eq. (12) to obtain the dimensionless value of \bar{t} .

$$\$ \bar{t} = \$1/\alpha_o^\# \text{ and } \tau_o^* = \$ \bar{t}. \quad (12)$$

Dividing the relation equation by α_o^* and substituting \bar{t} , it becomes $(\$1/\alpha_o^*)(1 - \beta_o^\#/\alpha_o^\#) = (1 - \beta_o^*/\alpha_o^*)$.

Because of Eq. (5) obtained $\$0 \leq (\alpha_o^\# - \beta_o^\#)$ and $\$0 \leq (\alpha_o^* - \beta_o^*)$, we have $0 \leq (1 - \beta_o^\#/\alpha_o^\#) \leq 1$ and $0 \leq (1 - \beta_o^*/\alpha_o^*) \leq 1$. Using $\tau_o^* = \$ \bar{t}$ in Step II, one should have the solutions $\alpha_o^* = \$1$ and $\beta_o^* \leq \$1$ to confirm the relation equation within the range of $(0, 1)$. $\Delta_o^{PT^*}$ should be within the range of $(\$0, \$1)$.

Therefore, the relative efficiency $E_o^{PT^*}$ is ensured between 0 and 1, as shown in Eq. (13).

$$0 < E_o^{PT^*} = \beta_o^*/\alpha_o^* \leq 1. \quad (13)$$

Certainly, normalizing Step I solutions to attain Step II solutions is a common practice in mathematical optimization problems. Eq. (14) likely represents this normalization process, where the Step I solutions are adjusted or transformed to achieve the solutions in Step II. This normalization might involve scaling or modifying Step I solutions to fulfill specific conditions required for Step II.

$$(\Delta_o^{PT^*}, \Delta_o^{PT\#}, v_o^*, u_o^*) = \bar{t} \times (\Delta_o^{PT\#}, \Delta_o^{PT\#}, v_o^\#, u_o^\#). \quad (14)$$

The symbol \mathcal{E}_o^{PT} denotes the set of *reference peers* DMU_o in the PT evaluations. DMU_j belongs to \mathcal{E}_o^{PT} has $\pi_{jo}^* > 0$ and is an efficient one. At the same time, the estimated intensity of the other inefficient DMU_j , $\pi_{jo}^* = 0$. DMU_o estimates the benchmark of each X_i and Y_r , \hat{x}_{io}^{PT*} and \hat{y}_{ro}^{PT*} via Eq. (15). DMU_o mimics reference peers with their estimated intensities, π_{jo}^* , $\forall j \in \mathcal{E}_o^{PT}$.

ix x xi

$$\begin{aligned}\hat{x}_{io}^{PT*} &= \sum_{\forall j \in \mathcal{E}_o^{PT}} x_{ij} \pi_{jo}^* = x_{io}(1 - q_{io}^*), \forall i \in I; \\ \hat{y}_{ro}^{PT*} &= \sum_{\forall j \in \mathcal{E}_o^{PT}} y_{rj} \pi_{jo}^* = y_{ro}(1 + p_{ro}^*), \forall r \in R.\end{aligned}\tag{15}$$

Assessing DMU_o with the adjusted X_i and Y_r , \hat{x}_{io}^{PT*} and \hat{y}_{ro}^{PT*} , as shown in Eq. (15), will have the PT efficiency \hat{E}_o^{PT} equals 1. Let the total of estimated intensities be the first SIC scalar, κ_o^1 , computed via Eq. (16).

$$\sum_{\forall j \in \mathcal{E}_o^{PT}} \pi_{jo}^* = \kappa_o^1.\tag{16}$$

Numerical example. In the columns of PT-I and PT-II of Table 2, summarized the solutions of Step I and Step II. The optimal values of τ_o , (v_o, u_o) , (v_{io}, u_{ro}) , and (α_j, β_j) are altered, while the other are unchanged. DMU_B and DMU_D are belong to \mathcal{E}_o^{PT} , while their intensities π_{oB}^* and π_{oD}^* are positive. The first SIC scalar is computed.

^{ix} Each DEA model used the same set of artificial goal weights to identify the reference peers for every DMU_o . The set of reference peers and DMU_o could have heterogeneous configurations of the observed dataset for more details ^{20 23 24}. To solve a VGA model, DMU_o systematically determines its unified goal price τ_o^* in two steps. It always identifies its homogeneous reference peers.

^x Halická and Trnovská⁸ listed objective functions and artificial goal weights used in several DEA Additive Models in Tables 2 and 3. The Additive CRS Models may obtain infeasible relative inefficiency F_o^* , which is not within the range (0,1) because the estimated $x_o^* v_o^* \neq 1$. However, the artificial goal weights in each model could not ensure that $x_o^* v_o^* = 1$. The Additive Models are unreliable and cannot be used.

^{xi} The slack-based-measure (SBM) model is a special one among the Additive Models; SBM models always have satisfactory results $0 \leq F_o^* (= f_o^*) < 1$. Therefore, SBM is the most frequently used method for EA.

Using a numerical example with multiple inputs and outputs to test those SBM models would find the result $F_o^* = f_o^* > (1 - y_o u_o^* / x_o v_o^*)$, the relative efficiency score $y_o u_o^* / x_o v_o^*$ was underestimated. Only if $x_o v_o^* = 1$ could satisfy the condition $F_o^* = f_o^* = (1 - y_o u_o^* / x_o v_o^*)$.

In SBM literature, the solutions v_o^* and u_o^* usually are not shown. The inaccurate SBM estimations will not be realized. For the original SBM models ^{25 26}, the development program aims to measure the efficiency score, which is a fractional expression. That led to the artificial goal weights in the multiplier program, $v_{io} \geq b_i^x [= 1/(m x_{io})]$ and $u_{ro} \geq b_r^y [= (x_o v_o - y_o u_o)/(s y_{ro})]$. Apparently, SBM models have inaccurate evaluations.

2.3. Technical and Scalar Choice (TSc) Model

Adding Eq. (20) to the PT-TAP program will have the bTSc-TAP program.

^{xii} Eq. (20) corresponds to the free-in-sign decision variable, $w_o(\$)$. Eqs. (18),(19), 20, and (21) construct the feasible region of the linear programming.

bTSc model, TAP (dual) program:

$$\Delta_o^{bTSc*}(\$) = \max_{q_o, p_o} \sum_{\forall i \in I} q_{io} \tau_o + \sum_{\forall r \in R} p_{ro} \tau_o, (\forall o \in J); \quad (17)$$

$$s.t. \sum_{\forall j \in J} x_{ij} \pi_{jo} + q_{io} x_{io} = x_{io}, \forall i \in I; \quad (18)$$

$$- \sum_{\forall j \in J} y_{rj} \pi_{jo} + p_{ro} y_{ro} = -y_{ro}, \forall r \in R; \quad (19)$$

^{xii} In DEA VRS models, the *convexity condition* is expressed as $\sum_{\forall j \in J} \lambda_{jo} = 1$ (see footnote i). While the CRS PPS polyhedral space does not include this convexity condition, the VRS PPS space incorporates it. The axioms of DEA theories are well established⁴⁷. Based on these theories and their graphical representations, each observed point corresponding to a DMU_o can adjust its single input and single output either by reduction or expansion. The resulting slacks, s_{1o}^x and s_{1o}^y project the point onto the efficient frontier of the envelope.

The envelopment analysis has been extended to the PPS, where DMUs operate with multiple inputs and outputs. This extension constitutes one of the fatal theoretical errors of DEA. The envelopment program of the Additive Model (see footnote vi) employs decision variables of slacks s_{io}^x and s_{ro}^y to measure the maximum relative inefficiency of DMU_o .

Based upon the DEA theory, the decision variables of intensities of DMUs $\lambda_{oj}, \forall j \in J$ in analyzing the PPS space are the same in analyzing the Additive Models⁴⁷. However, the two sets of intensities should be different. The Additive Model constructs a convex, feasible polyhedral space using hyperplanes and program conditions. In VGA models, use π_o as the variable intensities of DMUs. In the CRS (VRS) envelopment program, the absence (presence) of the condition $\sum_{\forall j \in J} \lambda_{jo} = 1$ distinguishes the CRS space from the VRS space. Importantly, this condition is not a convexity constraint within the convex space but rather a simple additional constraint. Adding this constraint reduces the CRS space to the VRS space. Implying the PPS convexity condition to the envelopment program introduces another fatal theoretical error in DEA.

The spaces defined by the PPS and the envelopment program differ significantly. The polyhedral PPS space comprises a finite set of points corresponding to the observed data. The reference peers of DMU_o are points situated on the piecewise linear PPS frontier, which cannot be represented either graphically or mathematically as a production function. In contrast, the feasible space of the envelopment program is a convex polyhedral space constructed using hyperplanes.

The optimal solution of the envelopment program is located at an extreme point, formed by the intersection of multiple hyperplanes and the objective function. Conversely, the projection point in the PPS space lies on the frontier, where the efficiency reference peers are situated. These points are distinct and are determined based on different criteria.

The envelopment programs for CRS Additive Models yield incomplete evaluations (see footnotes x and xi), as do those for VRS Additive Models⁸.

$$\sum_{\forall j \in J} \pi_{jo} = \kappa_o^c; \quad (20)$$

$$\pi_o, q_o, p_o \geq 0. \quad (21)$$

bTSc model, TVG (primal) program:

$$\Delta_o^{bTSc^*}(\$) = \min_{x_o, v_o, w_o} \sum_{\forall i \in I} v_{io} x_{io} - \sum_{\forall r \in R} u_{ro} y_{ro} + \kappa_o^c w_o, (\forall o \in J); \quad (22)$$

$$s.t. \sum_{\forall i \in I} v_{io} x_{ij} - \sum_{\forall r \in R} u_{ro} y_{rj} + 1w_o \geq 0(\$), \forall j \in J; \quad (23)$$

$$x_{io} v_{io} \geq \tau_o(\$), \forall i \in I; \quad (24)$$

$$y_{ro} u_{ro} \geq \tau_o(\$), \forall r \in R; \quad (25)$$

$$v_o, u_o, w_o \text{ free}. \quad (26)$$

In Eq. (22), the elements $(\kappa_o^c w_o^\#)$ and $(\kappa_o^c w_o^*)$ are repressed by the symbols $\omega_o^{c\#}$ and ω_o^{c*} , the *virtual scalar* $\$$ (*vScalar*) in Steps I and II.

As depicted in Eq. (27), γ_o and $(1 - \gamma_o)$ are the proportions of the total adjustment prices of inputs and outputs.^{xiii} If $w_o^\#$ (or w_o^*) equals \$0, let γ_o equal 0.5. Partition the *vScalar* into two parts to reflect the effects of the SIC on inputs and outputs of DMU_o . We denote them as *vScalar in inputs* (*ivScalar*) and *vScalar in outputs* (*ovScalar*); *vScalar* equals *ivScalar* plus *ovScalar*.

$$\gamma_o : (1 - \gamma_o) = \tau_o^\# \times \sum_{\forall i \in I} q_{io}^\# : \tau_o^\# \times \sum_{\forall r \in R} p_{ro}^\# = \tau_o^* \times \sum_{\forall i \in I} q_{io}^* : \tau_o^* \times \sum_{\forall r \in R} p_{ro}^*. \quad (27)$$

Eq. (28) is the expression of Eq. (22) in Step II, and the definitions of α_o^{c*} and β_o^{c*} . The symbols $\alpha_o^{c\#}$ and $\beta_o^{c\#}$ represent the two parts of $\Delta_o^{bTSc\#}$ in Step I. Usually, $\Delta_o^{bTSc\#}$ may exceed \$1. We gave several names for the mathematical terms in the equation.

$$\begin{aligned} \$0 \leq \Delta_o^{bTSc^*} &= v_o^* x_o - u_o^* y_o + \omega_o^{c*} = [v_o^* x_o + (1 - \gamma_o) \omega_o^{c*}] - (u_o^* y_o - \gamma_o \omega_o^{c*}) \\ &= [gvInput + ivScalar] - [gvOutput - ovScalar] \\ &= avInput - avOutput = \alpha_o^{c*} - \beta_o^{c*} \leq \$1; \\ \$0 \leq \Delta_o^{bTSc\#} &= v_o^\# x_o - u_o^\# y_o + \omega_o^{c\#} = [v_o^\# x_o + (1 - \gamma_o) \omega_o^{c\#}] - (u_o^\# y_o - \gamma_o \omega_o^{c\#}) \\ &= avInput - avOutput = \alpha_o^{c\#} - \beta_o^{c\#}. \end{aligned} \quad (28)$$

^{xiii} The multiplier program in each of the DEA Additive VRS Models, as noted in footnote vi, defines the optimal dimensionless relative inefficiency f_o^* as comprising three components: $x_o v_o^* - y_o u_o^* + 1 \times w_o^*$. However, the role of $1 \times w_o^*$ is not clearly defined. The convexity condition of the PPS is applied as the convexity condition for the feasible space of the Additive Model. This model assumes that f_o^* represents inefficiency. Nevertheless, the model encounters infeasible solutions⁸, as discussed in footnotes x and xi.

Instead, the minimized TVG $\Delta_o^{bTSc^*}$ in Eq. (23) is the virtual gap ($\$$). We partitioned TVG into two parts.

Similarly, Eq. (29) expressed the solutions of Eq. (23) in Step II are converted into two parts for each DMU_j , α_j^{c*} and β_j^{c*} . The estimated $vScalar$, $1w_o^*$ is decomposed into two components. The exact conversions are applied to the solutions of Step I.

$$\begin{aligned} \$0 \leq \Delta_j^{bTSc*} &= v_o^*x_j - u_o^*y_j + 1w_o^* \\ &= [v_o^*x_j + (1 - \gamma_o)1w_o^*] - (u_o^*y_j - \gamma_o1w_o^*) = \alpha_j^{c*} - \beta_j^{c*}, \forall j \in J. \end{aligned} \quad (29)$$

Each DMU_j is expressed by the pair of ($avInput$, $avOutput$), the virtual scales.

DMU-o determines its unified goal price, τ_o^* , to ensure Δ_o^{bTSc*} and $\Delta_o^{bTSc\#}$ are within the range of (\$0 and \$1). Eq. (28) supplied $(\alpha_o^{c\#}, \beta_o^{c\#})$ and $(\alpha_o^{c*}, \beta_o^{c*})$. The relationship $\tau_o^{\#} : \tau_o^* = 1 : \bar{t} = \Delta_o^{bTSc\#} : \Delta_o^{bTSc*}$ could be derived from the **relation equation** $(\bar{t}\alpha_o^{c\#} - \bar{t}\beta_o^{c\#}) = (\alpha_o^{c*} - \beta_o^{c*})$. Use Eq. (12) to obtain the dimensionless value of \bar{t} .

$$\bar{t} = \$1/\alpha_o^{c\#} = \$1/[v_o^{\#}x_o + (1 - \gamma_o)\omega_o^{c\#}]. \quad (30)$$

Dividing the relation equation by α_o^{c*} and substituting \bar{t} , we have $(\$1/\alpha_o^{c*})(1 - \beta_o^{c\#}/\alpha_o^{c\#}) = (1 - \beta_o^{c*}/\alpha_o^{c*})$.

Because of Eq. (28) obtained $\$0 \leq (\alpha_o^{c\#} - \beta_o^{c\#})$ and $\$0 \leq (\alpha_o^{c*} - \beta_o^{c*})$, we have $0 \leq (1 - \beta_o^{c\#}/\alpha_o^{c\#}) = (1 - \beta_o^{c*}/\alpha_o^{c*}) \leq 1$. Using $\tau_o^* = \$\bar{t}$ in Step II should have the solutions $\alpha_o^{c*} = \$1$ and $\beta_o^{c*} \leq \$1$ to confirm the relation equation within the range of (0,1). Then, DMU_o could ensure $\$0 \leq \Delta_o^{bTSc*} \leq \1 . DMU_o systematically determines the virtual unit prices (v_o^*, u_o^*) and virtual scales $(\alpha_j^{c*}, \beta_j^{c*})$ for each DMU_j .^{xiv} Therefore, as shown in Eq. (31), the relative efficiency E_o^{bTSc*} is ensured between 0 and 1.^{xv}

$$0 < E_o^{bTSc} = \frac{u_o^*y_o - \gamma_o\omega_o^{c*}}{v_o^*x_o + (1 - \gamma_o)\omega_o^{c*}} = \beta_o^{c*}/\alpha_o^{c*} \leq 1. \quad (31)$$

Normalizing the solutions of Step I by the dimensionless value \bar{t} would obtain the solutions of Step II, as shown in Eq. (32).

$$(\Delta_o^{bTSc*}, \Delta_o^{bTSc\#}, v_o^*, u_o^*, w_o^*) = \bar{t} \times (\Delta_o^{bTSc\#}, \Delta_o^{bTSc\#}, v_o^{\#}, u_o^{\#}, w_o^{\#}). \quad (32)$$

Use Eq. (33) to compute the benchmark of each X_i and Y_r , \hat{x}_{io}^{bTSc*} , and \hat{y}_{ro}^{bTSc*} . DMU_o imitates the reference peers with their estimated intensities, π_{jo}^* . DMU_o

^{xiv} In the Additive CRS and VRS Models, the estimated weights (v_o^*, u_o^*) are biased by the artificial goal weights (b_i^x, b_r^y) . In DEA literature, the virtual scales $(\alpha_o^{c*}, \beta_o^{c*})$ were not applied. However, the solutions (v_o^*, u_o^*) are not revealed.

^{xv} The DEA Additive VRS Models have infeasible solutions⁸, the reasons are addressed in footnotes x, xi, and xiii. Employing the PT model could obtain comprehensive solutions to the DEA CRS model. Using $\kappa_o^{bTSc} = 1$ to the bTSc model should have the DEA VRS comprehensive solutions.

would become efficient with the benchmarks.

$$\begin{aligned}\widehat{x}_{io}^{bTSc\star} &= \sum_{\forall j \in \mathcal{E}_o^{bTSc}} x_{ij} \pi_{jo}^* = x_{io}(1 - q_{io}^*), \forall i \in I; \\ \widehat{y}_{ro}^{bTSc\star} &= \sum_{\forall j \in \mathcal{E}_o^{bTSc}} y_{rj} \pi_{jo}^* = y_{ro}(1 + p_{ro}^*), \forall r \in R.\end{aligned}\quad (33)$$

Assess DMU_o with $\widehat{x}_{io}^{bTSc\star}$ and $\widehat{y}_{ro}^{bTSc\star}$ by the bTSc model will have $\Delta_o^{bTSc\star} = \$0$, and the bTSc efficiency $\widehat{E}_o^{bTSc\star}$ equals 1.

The symbol \mathcal{E}_o^{bTSc} denotes the set of reference peers in evaluating DMU_o by the bTSc model, where each reference DMU_j has $\pi_{jo}^* > 0$. The other inefficient DMU_j has $\pi_{jo}^* = 0$. In Eq. (29), any best DMU_j belongs to \mathcal{E}_o^{bTSc} has $\alpha_j^{c\star} = \beta_j^{c\star}$, while the other remaining DMUs have $\alpha_j^{c\star} > \beta_j^{c\star}$.

Numerical example. In the columns of TS1-I and TS1-II of Table 2, summarize the solutions in Step I and Step II. The first SIC scalar obtained in the PT model is used. The optimal values of τ_o (v_o, u_o), (v_{io}, u_{ro}), w_o , ω_o^c and (α_j, β_j) are altered, while the others are unchanged. The homogeneous reference peers DMU_B and DMU_D belong to \mathcal{E}_o^{TS1} , while their intensities π_{oB}^* and π_{oD}^* are positive. The comparisons between the columns of PT-II and TS-II are necessary.^{xvi}

In the columns of TS2-I and TS2-II of Table 2, DMU_o used the second SIC scalar and obtained the solutions in Phase-3. Comparing with the columns of TS1-I and TS1-II, we should find the solutions that have changed.

2.4. Duality Properties

We formulated VGA models based on the theories of linear programming⁴. Each money coin has two faces, while every linear programming model has primal and dual programs. Dualities are used to examine the correctness of the model formulations. In particular, the measurement units used for the parameters and decision variables should be consistent in the primal and dual programs.^{xvii} When the optimal TVG and TAP of the PT and bTSc models are equal, as stated in Eq. (34), it suggests an equilibrium or balance between the defined conditions or objectives within these models. This equality could signify an alignment between the total virtual gap and total slack price considerations, indicating a harmonized solution or relationship between the gap and price metrics.

$$\Delta_o^{PT\star}(\$) = \Delta_o^{PT\star}(\$) \quad \text{and} \quad \Delta_o^{bTSc\star}(\$) = \Delta_o^{bTSc\star}(\$). \quad (34)$$

^{xvi} SFA methods may suffer from the heterogeneous configurations of the dataset, making it a challenging task to identify outliers. SFA estimates the average production frontier for each dependent (output, Y_r) and m independent (inputs) of the n DMUs. In contrast, VGA models assess DMU_o with m inputs and s outputs simultaneously, considering its reference peers rather than relying on the average production frontier.

^{xvii} In DEA literature, many proposed DEA models do not offer the multiplier program and its solutions. As a result, the dualities of those models cannot be examined. Additionally, the formulations of these DEA models are dimensionless²⁷.

The strong complementary slackness conditions of the two VGA models are shown in Eq. (35) and Eq. (36).

$$\left[\sum_{\forall j \in \mathcal{E}_o^{VGA}} x_{ij} \pi_{jo}^* - x_{io}(1 - q_{io}^*) \right] v_{io}^* = \$0, \forall i \in I. \quad (35)$$

$$\left[\sum_{\forall j \in \mathcal{E}_o^{VGA}} (y_{rj} \pi_{jo}^*) - y_{ro}(1 + p_{ro}^*) \right] u_{ro}^* = \$0, \forall r \in R. \quad (36)$$

v_o and u_o are free-in-signs in the TVG programs. Since $(X, Y) > 0$ and $\tau_o^* > \$0$ yields the estimated virtual unit prices, $v_o^* > 0, u_o^* > 0$. Therefore, the braces at the left-hand side of Eq. (35) and Eq. (36) equal zero. In other words, DMU_o does not need to perform the sensitivity analysis on the parameters in the model (x_o, y_o) . The VGA models obtained robust estimations of p_{io}^* and q_{ro}^* so that DMU_o ensued to project on the *b-Efficiency Equator*, see Figures 3 through 6. ^{xviii}

For the PT model, each DMU_j has the property as shown in Eq. (37). When $(v_o^* x_j - u_o^* y_j) = 0$, DMU_j belongs to \mathcal{E}_o^{PT} and $\pi_{jo}^* > 0$. The *b-Efficiency Equator* is the diagonal line at the origin in Figure 3, $(v_o^* x_j - u_o^* y_j) = \$0, \forall j \in \mathcal{E}_o^{PT}$.

$$(v_o^* x_j - u_o^* y_j) \pi_{jo}^* = \$0, \forall j \in J. \quad (37)$$

For the bTSc model, each DMU_j has the property shown in Eq. (38). w_o^* which is the estimated unit price of the SIC scalar and $\kappa_o^c w_o^*$ is the *vScalar*. When $(v_o^* x_j - u_o^* y_j + 1w_o^*) = \0 , DMU_j belongs to \mathcal{E}_o^{bTSc} and $\pi_{jo}^* > 0$. Otherwise, $(v_o^* x_j - u_o^* y_j + 1w_o^*) > \0 , DMU_j does not belong to \mathcal{E}_o^{bTSc} and $\pi_{jo}^* = 0$. The *b-Efficiency Equator* is the diagonal line at the origin in Figure 4, $(v_o^* x_j - u_o^* y_j + 1w_o^*) = \$0, \forall j \in \mathcal{E}_o^{bTSc}$.

$$(v_o^* x_j - u_o^* y_j + w_o^*) \pi_{jo}^* = \$0, \forall j \in J. \quad (38)$$

Eq. (39) depicts the relationships between the estimated decision variables in the TVG and TAP programs.

$$(v_{io}^* x_{io} - \tau_o^*) q_{io}^* = \$0, \forall i \in I; (u_{ro}^* y_{ro} - \tau_o^*) p_{ro}^* = \$0, \forall r \in R. \quad (39)$$

In Eq. (40), $\sum_{\forall j \in \mathcal{E}_o^{bTSc}} \pi_{jo}^* - \kappa_o^c = 0$ the TVG of the bTSc model is decreased, constant, and increased when $w_o^* > \$0, w_o^* = \0 , and $w_o^* < \$0$ respectively.

$$\left(\sum_{\forall j \in \mathcal{E}_o^{bTSc}} \pi_{jo}^* - \kappa_o^c \right) w_o^* = \$0. \quad (40)$$

2.5. Post-Analysis of the Optimal Solutions

The optimal solutions from the PT and bTSc models have the ability to quantify the assessment items.

^{xviii} Using each existing DEA Additive CRS and VRS Model to evaluate each DMU_o in the PPS with multiple inputs and outputs should provide a similar 2D graphical representation to demonstrate the solutions. The adjusted DMU_o should have a relative efficiency score of 1 and should project onto the *b-Efficiency Equator*. However, the 2D figure may reveal that the DEA model provides incomplete evaluations. In contrast, VGA models have been verified to offer comprehensive evaluations, as demonstrated in Figures 3 through 6.

2.5.1. Virtual Technology Sets

The formulation and definitions of the *virtual technology set* in the context of Step II within the PT and bTSc models are presented in Eq. (41) and Eq. (42). Step I has similar expressions. In Eq. (41) and Eq. (42), the virtual scales of each DMU_j ($vInput, vOutput$) and ($avInput, avOutput$) are defined in Eq. (12) and Eq. (28). The virtual scales in Step I for each DMU_j represent certain aspects or characteristics within the model. These sets likely encapsulate specific parameters, constraints, or variables pertinent to the subsequent steps' formulation and computation. Virtual scales in Step II might represent refined or adjusted versions of the initial sets of Step I, potentially incorporating the outcomes or adjustments derived from the earlier steps.

The transition from Step I to Step II usually involves refining or re-calibrating the parameters or sets based on the intermediate solutions or computations from the preceding step. This iterative process often helps converge toward more accurate or optimal results within the models.

$$\Phi_o^{PT*} = \{(\alpha^*, \beta^*) \mid (\alpha_j^*, \beta_j^*), \forall j \in J\}. \quad (41)$$

$$\Phi_o^{bTSc*} = \{(\alpha^{c*}, \beta^{c*}) \mid (\alpha_j^{c*}, \beta_j^{c*}), \forall j \in J\}. \quad (42)$$

2.5.2. Return-to-virtual-scale (RTvS)

Eq. (43) and Eq. (44) depict the computation steps for *benchmark virtual scales* and *affected benchmark virtual scale* in the PT and bTSc models during Step II ($bvInput, bvOutput$) = $(\hat{\alpha}_o^*, \hat{\beta}_o^*)$ and ($abvInput, abvOutput$) = $(\hat{\alpha}_o^{c*}, \hat{\beta}_o^{c*})$, respectively. These equations likely involve transforming or deriving benchmark values based on specific conditions or constraints within the models. ^{xix}

The expressions for $bvInput, bvOutput, abvInput, and abvOutput$ in Step I are similar to those in Eq. (43) and Eq. (44) with the replacement of the superscript " \star " with " $\#$." This step-wise process of deriving and refining benchmarks could indicate a progressive approach where the initial estimates from Step I are further modified or calibrated in Step II based on additional considerations or parameters introduced in the models.

$$\hat{\alpha}_o^* = \sum_{\forall i \in I} \hat{x}_{io} v_{io}^* \text{ and } \hat{\beta}_o^* = \sum_{\forall r \in R} \hat{y}_{ro} u_{ro}^*. \quad (43)$$

$$\hat{\alpha}_o^{c*} = [v_o^* \hat{x}_o + (1 - \gamma_o) \omega_o^{c*}]; \hat{\beta}_o^{c*} = (u_o^* \hat{y}_o - \gamma_o \omega_o^{c*}). \quad (44)$$

^{xix}The virtual scale of each DMU is represented as a point on the 2D graphical intuition used to evaluate DMU_o . For example, Figures 3 and 4 show that the DMUs are located either beneath or on the b-Efficiency Equator when evaluating DMU_K . DEA models, however, cannot effectively express the PPS and its envelope. As a result, the points corresponding to efficient DMUs, as well as the projection point of DMU_o , may not lie on *b-Efficiency Equator*.

Eq. (45) and Eq. (46) compute the RTvS, (Ξ_o^{PT*} and Ξ_o^{bTSc*}), is based on the virtual scales. The RTvS values might represent a measure or index that assesses the efficiency or productivity performance DMU_o within the context of these specific models. ^{xx}

$$\Xi_o^{PT*} = (\widehat{\beta}_o^*/\beta_o^*)/(\widehat{\alpha}_o^*/\alpha_o^*) = 1/E_o^{PT*}. \quad (45)$$

$$\Xi_o^{bTSc*} = (\widehat{\beta}_o^{c*}/\beta_o^{c*})/(\widehat{\alpha}_o^{c*}/\alpha_o^{c*}) = 1/E_o^{bTSc*}. \quad (46)$$

For the case that $\omega_o^* \geq \$0$, Ξ_o^{bTSc*} and E_o^{bTSc*} will be decreased and increased as the SIC scalar κ_o^c rises. Conversely, when $\omega_o^* \leq \$0$, Ξ_o^{bTSc*} and E_o^{bTSc*} will be decreased and increased, respectively, as the SIC scalar κ_o^c diminishes. A preference is given to higher Ξ_o^{bTSc*} and E_o^{bTSc*} . Depending on whether $\omega_o^* \geq \$0$ or $\omega_o^* \leq \$0$, DMU_o has the flexibility to adjust κ_o^c towards its lower or upper bound. This adjustment aims to achieve the final κ_o^z that encompasses achievable benchmarks for inputs and outputs. The implications of these dynamics are further elucidated through the numerical examples and graphical illustrations presented in Section 5.1, which depict how varying κ_o^c influences the efficiency and the position of DMU_o relative to the b-Efficiency Equator. ^{xxi}

2.5.3. Interconnections Between Inputs and Outputs Indices

Eq. (47) and Eq. (48) demonstrate adjustments to the affected virtual prices of an input ($v_{io}^*x_{io} + \gamma_{io}^Q\omega_o^{c*}$), and an output ($u_{ro}^*y_{ro} - \gamma_{ro}^P\omega_o^{c*}$), respectively, considering the proportions to the vScalar, represented by γ_{io}^Q and γ_{ro}^P .

$$\Delta_o^{bTSc*} = \sum_{\forall i \in I} (v_{io}^*x_{io} + \gamma_{io}^Q\omega_o^{c*}) - \sum_{\forall r \in R} (u_{ro}^*y_{ro} - \gamma_{ro}^P\omega_o^{c*}). \quad (47)$$

$$\gamma_{io}^Q = (1 - \gamma_o)q_{io}^*/ \sum_{\forall i \in I} q_{io}^*, \forall i \in I; \quad (48)$$

$$\gamma_{ro}^P = \gamma_o p_{ro}^*/ \sum_{\forall r \in R} p_{ro}^*, \forall r \in R.$$

In Eq. (47) and Eq. (48), the proportions involving ($v_{io}^*x_{io} + \gamma_{io}^Q\omega_o^{c*}$) and ($u_{ro}^*y_{ro} - \gamma_{ro}^P\omega_o^{c*}$) indeed highlight the interconnectedness between the input and output indices. These proportions indicate the adjustments made to the affected

^{xx} The concepts of scale elasticity and returns to scale in the nonparametric methodology of DEA are crucial characteristics of a production function ²⁸. The authors of DEA models assume the existence of a linear production frontier for DMU_o . In contrast, the bTSc and sTSc VGA models do not focus on the production function of the PPS. Instead, they measure the return-to-virtual-scale of DMU_o .

^{xxi} Tables 2 and 3 listed the returns-to-virtual-scale of DMU_o . DEA models could not compute the return-to-scale, which is a concept that arises in the context of firms' production function in economics. Depending on the sign of the estimated w_o^* , DMU_o exhibits decreasing or increasing return-to-scale.

virtual prices concerning the quantities represented by γ_{io}^Q and γ_{ro}^P , display how changes in one influence the other within the context of the model variables and constraints.

2.5.4. 2D Graphic Intuitions

DMU-o can visualize the outcomes of the post-analysis based on the optimal solutions from the VGA models. For instance, we use the example dataset in Table 1. One can identify the third SIC scalar κ_o^3 by try and error. While the κ_o^3 may not be within the range of κ_o^1 and κ_o^2 . The particular κ_o^3 within the TS3 model produces $E_o^{PT^*} = E_o^{TS3^*}$. Pure technical efficiency is affected by the SIC. The exact evaluations of PT and TS3 models are demonstrated in Figure 3, in which the *b-Efficiency Equator* should not be viewed as the efficiency frontier.

The *anchor point*^{xxii} of the bTSc model is represented by *APc*, where "c" denotes the choices 1, 2, and 3. Points Kp, K3, AP3, and O are located at (α_o^*, β_o^*) , $(\alpha_o^{3*}, \beta_o^{3*})$, $([1 - \gamma_o]\omega_o^{3*}, -\gamma_o\omega_o^{3*})$, and (0,0), respectively. Points O, K3, and AP3 are located at the corners of the triangle. The upper-right of the figure shows the two rectilinear distances between the pair points (Kp, Tp) and (K3, T3), the virtual gaps estimated by the PT and TS3 models. *DMU_o* could comprehend the results between the PT and TS3 models to understand the effects of the SIC.

Similarly, in Figure 4, Points O, K1, and AP1 of the triangle are solutions of the TS1 model. The three points O, K2, and AP2 at the triangle are solutions of the TS2 model. Figure 4 showcases the effects of using different SIC scalars within a certain interval and helping select a final scalar κ_o^z for productivity management. In this example, due to $w_o^* > 0$, we have $E_o^{TS2^*} > E_o^{bTSz^*} > E_o^{TS1^*}$. The bTSz model provides the most preferred (q_o, p_o) ($q_o^{bTSz^*}, p_o^{bTSz^*}$).

In Figure 4, Points O, APc, and Kc at the triangle express solutions of the bTSc

^{xxii} Banker et al.²⁹ used Figure 3 to illustrate the specific VRS PPS with one input (x) and one output (y). The line segments passing through points A and E represent increasing and decreasing returns to scale, as indicated by the sign of w_o^* . Each line intersects the vertical and horizontal axes at a distance of $-w_o^*$, measured in the same units as x and y. For PPS with multiple inputs and outputs, w_o^* becomes dimensionless. See footnote vi, the multiplier program⁸ of the Additive VRS Models normalizes input and output values to ensure compatibility with the dimensionless w_o^* , a dual variable associated with the convexity condition. Additional details can be found in footnote xiii.

Linear programming-based DEA models define decision variables and coefficients as dimensionless. However, this process disrupts the fundamental conditions of problem formulations, making it impossible to verify DEA models through duality.

Each DEA model could not demonstrate the value of w_o^* on a graph. In each bTSc and sTSc VGA model, the anchor point is located on one of the axes of the 2D graphical intuition with intercept $\omega_o^*(\$)$. The actual measurement of the returns to scale in practice relies on the concept of *scale elasticity* and scale efficiency, see Page 31 in Sickles and Zelenyuk⁷. However, no one in the DEA literature has presented a solution for multiple inputs and outputs.

model. Eq. (49), Eq. (50), and Eq. (51) are the expressions of the slopes for the vectors $\overrightarrow{O, Kc}$, $\overrightarrow{O, APc}$, and $\overrightarrow{APc, Kc}$, respectively. The ratio of the scalar prices of inputs to outputs equals the slope $\bar{m}(\overrightarrow{O, APc})$. Similarly, the ratio of the *gray virtual input to output* equals the slope $\bar{m}(\overrightarrow{APc, Kc})$.

$$\bar{m}(\overrightarrow{O, Kc}) = \frac{\beta_o^{c*} - 0}{\alpha_o^{c*} - 0} = \frac{\beta_o^{c*}}{\alpha_o^{c*}}. \quad (49)$$

$$\bar{m}(\overrightarrow{O, APc}) = \frac{-\gamma_o \omega_o^{c*} - 0}{(1 - \gamma_o) \omega_o^{c*} - 0} = \frac{-\gamma_o \omega_o^{c*}}{(1 - \gamma_o) \omega_o^{c*}}. \quad (50)$$

$$\bar{m}(\overrightarrow{APc, Kc}) = \frac{\beta_o^{c*} - (-\gamma_o \omega_o^{c*})}{\alpha_o^{c*} - [(1 - \gamma_o) \omega_o^{c*}]} = \frac{u_o^* y_o}{v_o^* x_o}. \quad (51)$$

For instance, in Figure 3, the triangle of the TS3 model has the following expressions.

$$\overrightarrow{O, K3} = \overrightarrow{O, AP3} + \overrightarrow{AP3, K3} \iff \frac{\beta_o^{3*}}{\alpha_o^{3*}} = \frac{u_o^* y_o - \gamma_o \omega_o^{3*}}{v_o^* x_o + (1 - \gamma_o) \omega_o^{3*}}. \quad (52)$$

As shown in Eq. (53), the estimated bTSc efficiency score could be visualized as the relationships of the three vectors.

$$\overrightarrow{O, Kc} = \overrightarrow{O, APc} + \overrightarrow{APc, Kc}; \quad E_o^{bTSc*} = \bar{m}(\overrightarrow{O, Kc}) = \frac{\beta_o^{c*}}{\alpha_o^{c*}}. \quad (53)$$

The effects of the SIC within the bTSc model could be visualized as triangular with points O, APc, and Kc in the 2D graphical intuition. The slopes $\bar{m}(\overrightarrow{O, APc})$ and $\bar{m}(\overrightarrow{APc, Kc})$ are not the scale and technical efficiencies.

3. Scenario-II: Evaluating the Super-Efficiency

Figure 1 shows that Scenario II computes the super-efficiency. The PT and bTSc models are modified into sPT and sTEc models. When the efficient DMU_o expands inputs and deduces outputs, its super-efficiency will be reduced to 1. In particular, DMU_o is excluded from the reference set J when assessing its super-efficiency.

3.1. *super-Pure Technical Efficiency (sPT) Model*

sPT model, TAP (dual) program: ^{xxiii}

$$\delta_o^{sPT*} = \min_{q_o, p_o, \pi_o} \sum_{\forall i \in I} q_{io} \tau_o + \sum_{\forall r \in R} p_{ro} \tau_o; \quad (54)$$

^{xxiii} Liu et al. ³⁰ reviewed slack-based measure of CRS efficiency and super-efficiency models. They attempted to tackle the existing problems in measuring the CRS super-efficiency. They offered two envelopment programs but without the multiplier programs. The SBM-based super-efficiency measurement models could not correctly evaluate several DMU_o , see footnote xi for the same reasons. Instead, using the sPT model could obtain the comprehensive assessments.

$$s.t. - \sum_{\forall j \in J - \{o\}} x_{ij}\pi_{jo} + q_{io}x_{io} \geq -x_{io}, \forall i \in I; \quad (55)$$

$$\sum_{\forall j \in J - \{o\}} y_{rj}\pi_{jo} + p_{ro}y_{ro} = y_{ro}, \forall r \in R; \quad (56)$$

$$\pi_o, q_o, p_o \geq 0. \quad (57)$$

sPT model, TVG (primal) program:

$$\Delta_o^{sPT*} = \max_{v_o, u_o} - \sum_{\forall i \in I} v_{io}x_{io} + \sum_{\forall r \in R} u_{ro}y_{ro}; \quad (58)$$

$$s.t. - \sum_{\forall i \in I} v_{io}x_{ij} + \sum_{\forall r \in R} u_{ro}y_{rj} \leq 0, \forall j \in J - \{o\}; \quad (59)$$

$$x_{io}v_{io} \geq \tau_o, \forall i \in I; \quad (60)$$

$$y_{ro}u_{ro} \geq \tau_o, \forall r \in R; \quad (61)$$

$$v_o \geq 0 \text{ and } u_o \text{ free.} \quad (62)$$

Similar to Eq. (10) and Eq. (11), the optimal solutions of Eq. (54) and Eq. (58) as depicted in Eq. (63) and Eq. (64). Usually, $\Delta_o^{sPT\#}$ in Step I exceeds \$1.

$$\$0 < \delta_o^{sPT\#} = \sum_{\forall i \in I} q_{io}^{\#} \times \$1 + \sum_{\forall r \in R} p_{ro}^{\#} \times \$1 = \Delta_o^{sPT\#}; \quad (63)$$

$$\$0 < \delta_o^{sPT*} = \sum_{\forall i \in I} q_{io}^* \tau_o^* + \sum_{\forall r \in R} p_{ro}^* \tau_o^* = \delta_{xo}^{sPT*} + \delta_{yo}^{sPT*} = \Delta_o^{sPT*} < \$1.$$

$$\$0 < \Delta_j^{sPT\#} = -v_o^{\#} x_j + u_o^{\#} y_j = -\alpha_j^{\#} + \beta_j^{\#}; \quad (64)$$

$$\$0 < \Delta_j^{sPT*} = -v_o^* x_j + u_o^* y_j = -\alpha_j^* + \beta_j^* \leq \$1.$$

DMU-o determines its unified goal price τ_o^* to ensure δ_o^{sPT*} and $= \Delta_o^{sPT*}$ in Step II are within the range (\$0, \$1). Eq. (64) supplied $(\alpha_o^{\#}, \beta_o^{\#})$ and (α_o^*, β_o^*) . The relationship $\tau_o^{\#} : \tau_o^* = 1 : \bar{t} = \Delta_o^{sPT\#} : \Delta_o^{sPT*}$ could be derived from the *relation equation* $\bar{t}(-\alpha_o^{\#} + \beta_o^{\#}) = 1(-\alpha_o^* + \beta_o^*)$. Use Eq. (65) to obtain the dimensionless value of \bar{t} .

$$\bar{t} = \$1/\beta_o^{\#} \text{ and } \tau_o^* = \$\bar{t}. \quad (65)$$

Dividing the relation equation by β_o^* substituting it \bar{t} , we have the new relation equation $(1/\beta_o^*)(-\alpha_o^{\#}/\beta_o^{\#} + 1) = (-\alpha_o^*/\beta_o^* + 1)$.

Because of Eq. (58) obtained $\$0 \leq (-\alpha_o^{\#} + \beta_o^{\#})$ and $\$0 \leq (-\alpha_o^* + \beta_o^*)$, we have $0 \leq (-\alpha_o^{\#}/\beta_o^{\#} + 1)$ and $0 \leq (-\alpha_o^*/\beta_o^* + 1)$. Using $\tau_o^* = \$\bar{t}$ in Step II, should have the solutions $\beta_o^* = \$1$ and $\alpha_o^* < \$1$ to confirm $(-\alpha_o^{\#}/\beta_o^{\#} + 1) = (-\alpha_o^{\#}/\beta_o^{\#} + 1)$ and $\$0 \leq \Delta_o^{sPT*}$. The relative super-efficiency in Step I and Step II should be equal, as depicted in Eq. (66).

$$1 \leq E_o^{sPT} = \beta_o^{\#}/\alpha_o^{\#} = \beta_o^*/\alpha_o^*. \quad (66)$$

Numerical example. The columns of B sPT-II and D sPT-II in Table 3 summarized the evaluation solutions of DMU_B and DMU_D in Step II. The two efficient

DMUs have different reference sets, (DMU_A) and (DMU_B, DMU_G) . The super-efficiencies exceeded 1. The primal and dual programs of the sPT VGA model provide comprehensive evaluations. DMU_B has the lowest value of Y_1 567, and its super-efficiency E_B^{sPT} equals 2.4126. DMU_D has the highest value of X_1 281, and its super-efficiency E_D^{sPT} equals 1.3533. ^{xxiv}

Eq. (67) likely represents this normalization process, where the Step I solutions are adjusted or transformed to achieve the solutions in Step II.

$$(\delta_o^{sPT*}, \Delta_o^{sPT*}, v_o^*, u_o^*) = \bar{t} \times (\delta_o^{sPT\#}, \Delta_o^{sPT\#}, v_o^\#, u_o^\#). \quad (67)$$

The symbol \mathcal{E}_o^{sPT} denotes the reference set of DMU_o in the sPT evaluations. Each peer DMU_j belonging to the reference set has sPT efficiency equal to 1 and its estimated intensity $\pi_{jo}^* > 0$. At the same time, the estimated intensity of the other inefficient DMUs, $\pi_{jo}^* = 0$. DMU_o estimates the benchmark of each X_i and Y_r , \hat{x}_{io}^{sPT*} and \hat{y}_{ro}^{sPT*} via Eq. (68). DMU_o mimics the reference peers with their estimated intensities, $\pi_{jo}^*, \forall j \in \mathcal{E}_o^{sPT}$. DMU_o is superior to its reference peers, whose criteria configurations are analog to DMU_o .

$$\begin{aligned} \hat{x}_{io}^{sPT*} &= \sum_{\forall j \in \mathcal{E}_o^{sPT}} x_{ij} \pi_{jo}^* = x_{io}(1 + q_{io}^*), \forall i \in I; \\ \hat{y}_{ro}^{sPT*} &= \sum_{\forall j \in \mathcal{E}_o^{sPT}} y_{rj} \pi_{jo}^* = y_{ro}(1 - p_{ro}^*) \forall r \in R. \end{aligned} \quad (68)$$

Assessing DMU_o with the adjusted X_i and Y_r , \hat{x}_{io}^{sPT*} and \hat{y}_{ro}^{sPT*} , as shown in Eq. (68), will have the sPT efficiency \hat{E}_o^{sPT} equals 1.

$$\sum_{\forall j \in \mathcal{E}_o^{sPT}} \pi_{jo}^* = \kappa_o^1. \quad (69)$$

Let the total estimated intensities be the first SIC scalar κ_o^1 , computed via Eq. (69).

3.2. Super-technical and Scalar choice Efficiency (sTSc) Model

^{xxv} Adding the SIC Eq. (73) to the sPT-TAP program will have the sTSc-TAP program. The SIC corresponds to the free-in-sign decision variable w_o . Choose the SIC scalar κ_o^c to assess its super-efficiency DMU_o .

sTSc model, TAP (dual) program:

^{xxiv} DEA Additive Models could not measure the CRS efficiency; see footnotes x and xi for the reasons. The existing Additive Models to measure the CRS super-efficiency do not verify the solutions by examining the dualities.

^{xxv} Chen et al.³¹ provided comprehensive reviews of VRS super-efficiency SBM-based models. They presented the two envelopment programs without the multiplier programs. Footnote xi discussed the same reasons the two envelopment programs have incomplete evaluations. Instead, using $\kappa_o^{sTSc} = 1$ to the sTSc model could obtain the comprehensive assessments.

$$\delta_o^{sTSc*} = \min_{q_o, p_o} \sum_{\forall i \in I} q_{io} \tau_o + \sum_{\forall r \in R} p_{ro} \tau_o; \quad (70)$$

$$s.t. - \sum_{\forall j \in J - \{o\}} x_{ij} \pi_{jo} + q_{io} x_{io} \geq -x_{io}, \forall i \in I; \quad (71)$$

$$\sum_{\forall j \in J - \{o\}} y_{rj} \pi_{jo} + p_{ro} y_{ro} = y_{ro}, \forall r \in R; \quad (72)$$

$$\sum_{\forall j \in J - \{o\}} \pi_{jo} = \kappa_o^c; \quad (73)$$

$$\pi_o, q_o, p_o \geq 0. \quad (74)$$

sTSc model, TVG (primal) program:

$$\Delta_o^{sTSc*} = \max_{x_o, v_o, w_o} - \sum_{\forall i \in I} v_{io} x_{io} + \sum_{\forall r \in R} u_{ro} y_{ro} + \kappa_o^c w_o; \quad (75)$$

$$s.t. - \sum_{\forall i \in I} v_{io} x_{ij} + \sum_{\forall r \in R} u_{ro} y_{rj} + 1w_o \leq 0, \forall j \in J - \{o\}; \quad (76)$$

$$x_{io} v_{io} \geq \tau_o, \forall i \in I; \quad (77)$$

$$y_{ro} u_{ro} \geq \tau_o, \forall r \in R; \quad (78)$$

$$v_o \geq 0, u_o, w_o \text{ free}. \quad (79)$$

Similar to the bTSc model, the sTSc model determines the unified goal price in two steps. $\tau_o^\# = \$1$ and $\tau_o^* = \bar{\$}$ will solve the TAP program comprehensively with the solutions $(q_o^*, p_o^*, \pi_o^*) = (q_o^\#, p_o^\#, \pi_o^\#)$. Use Eq. (27) to obtain γ_o and $(1 - \gamma_o)$. Partition the *vScalar* into two parts to reflect the effects of the SIC on inputs and outputs *DMU_o*.

The maximized Δ_o^{sTSc} of *DMU_o* in Step II of Eq. (75) is expressed as the *affected virtual Output (avOutput)* minus *affected virtual Input (avInput)*, $-\alpha_o^{c*} + \beta_o^{c*}$, as shown in Eq. (80). The solutions in Step I have a similar expression, $-\alpha_o^{c\#} + \beta_o^{c\#}$. Usually, in Step I $\Delta_o^{sTSc\#}$ exceeds $\$1$.

$$\begin{aligned} \$0 &\leq \Delta_o^{sTSc*} = -v_o^* x_o + u_o^* y_o + \omega_o^{c*} \\ &= -[v_o^* x_o - (1 - \gamma_o) \omega_o^{c*}] + (u_o^* y_o + \gamma_o \omega_o^{c*}) \\ &= -[gvInput - ivScalar] + [gvOutput + ovScalar] \\ &= -avInput + avOutput = -\alpha_o^{c*} + \beta_o^{c*} \leq \$1; \\ \$0 &\leq \Delta_o^{sTSc\#} = -\alpha_o^{c\#} + \beta_o^{c\#}. \end{aligned} \quad (80)$$

Eq. (81) expresses the solution of Eq. (76) of each remaining *DMU_j* $-\alpha_j^{c*} + \beta_j^{c*}$ in Step II. Similarly, the solution of Step I is $-\alpha_j^{c\#} + \beta_j^{c\#}$. The estimated *vScalar* of Step II in Eq. (76), $1w_o^*$, is decomposed into two components.

$$\begin{aligned} \$0 &< \Delta_j^{sTSc*} = -v_o^* x_j + u_o^* y_j + 1w_o^* \\ &= -[v_o^* x_j - (1 - \gamma_o) 1w_o^*] + (u_o^* y_j + \gamma_o 1w_o^*) = -\alpha_j^{c*} + \beta_j^{c*}, \forall j \in J, j \neq o. \end{aligned} \quad (81)$$

Each *DMU_j* is expressed by the pair of (*avInput*, *avOutput*), called as *virtual scales*.

DMU-o determines its unified goal price, τ_o^* which is to ensure $\delta_o^{sTSc^*}$ and $\Delta_o^{sTSc^*}$, in Step II, falls into the range of ($\$0, \1). Eq. (80) supplied $(\alpha_o^{c\#}, \beta_o^{c\#})$ and $(\alpha_o^{c^*}, \beta_o^{c^*})$. The relationship $\tau_o^* : \tau_o^* = 1 : \bar{t} = \Delta_o^{sTSc\#} : \Delta_o^{sTSc^*}$ could be derived from the relation equation $\bar{t}(-\alpha_o^{c\#} + \beta_o^{c\#}) = 1(-\alpha_o^{c^*} + \beta_o^{c^*})$. Use Eq. (82) to obtain the dimensionless value of \bar{t} .

$$\bar{t} = \$1/\beta_o^{c\#} = \$1/(u_o^\# y_o + \gamma_o \omega_o^{c\#}) = \tau_o^*. \quad (82)$$

Dividing the relative equation by $\beta_o^{c^*}$ and substituting \bar{t} , we have the new relation equation $1/\beta_o^{c^*} (-\alpha_o^{c\#}/\beta_o^{c\#} + 1) = (-\alpha_o^{c^*}/\beta_o^{c^*} + 1)$.

Because of Eq. (80) obtained $\$0 \leq (-\alpha_o^{c\#} + \beta_o^{c\#})$ and $\$0 \leq (-\alpha_o^{c^*} + \beta_o^{c^*}) \leq \1 . Using $\tau_o^* = \$\bar{t}$ Step II, should have the solutions $\beta_o^{c^*} = \$1$, and $\alpha_o^{c^*} \leq \$1$, to confirm $(-\alpha_o^{c\#}/\beta_o^{c\#} + 1) = (-\alpha_o^{c^*}/\beta_o^{c^*} + 1)$. Therefore, we have $\$0 \leq \Delta_o^{sTSc^*} \leq \1 . Eq. (83) shows the relative super-efficiency $E_o^{sTSc^*}$.

$$0 < E_o^{sTSc} = \frac{u_o^* y_o + \gamma_o \omega_o^{c^*}}{-v_o^* x_o + (1 - \gamma_o) \omega_o^{c^*}} = \beta_o^{c^*} / \alpha_o^{c^*}. \quad (83)$$

Normalizing the solutions of Step I by the dimensionless value \bar{t} would obtain the solutions of Step II, as shown in Eq. (84).

$$(\Delta_o^{sTSc^*}, \delta_o^{sTSc^*}, v_o^*, u_o^*, w_o^*) = \bar{t} \times (\Delta_o^{sTSc\#}, \delta_o^{sTSc\#}, v_o^\#, u_o^\#, w_o^\#). \quad (84)$$

The symbol \mathcal{E}_o^{sTSc} denotes the set of reference peers in evaluating DMU_o by the sTSc model, where each reference peer DMU_j has $\pi_{j_o}^* > 0$. The other inefficient DMU_j has $\pi_{j_o}^* = 0$. In Eq. (81), any best DMU_j belongs to \mathcal{E}_o^{sTSc} has $\alpha_j^{c\#} = \beta_j^{c\#}$ and $\alpha_j^{c^*} = \beta_j^{c^*}$, while the other remaining DMUs have $\alpha_j^{c\#} > \beta_j^{c\#}$ and $\alpha_j^{c^*} > \beta_j^{c^*}$.

Use Eq. (85) to compute the benchmarks of X_i and Y_r , $\hat{x}_{i_o}^{sTSc^*}$, and $\hat{y}_{r_o}^{sTSc^*}$. DMU_o imitates the reference peers with their estimated intensities ($\pi_{j_o}^*$).

DMU_o uses the benchmarks, $\hat{x}_{i_o}^{sTSc^*}$ and $\hat{y}_{r_o}^{sTSc^*}$, will decrease the sTSc super-efficiency \hat{E}_o^{sTSc} to 1 while the $\delta_o^{sTSc^*}$ drops to $\$0$.

$$\begin{aligned} \hat{x}_{i_o}^{sTSc^*} &= \sum_{\forall j \in \mathcal{E}_o^{sTSc}} x_{ij} \pi_{j_o}^* = x_{i_o} (1 + q_{i_o}^*), \forall i \in I; \\ \hat{y}_{r_o}^{sTSc^*} &= \sum_{\forall j \in \mathcal{E}_o^{sTSc}} y_{rj} \pi_{j_o}^* = y_{r_o} (1 - p_{r_o}^*), \forall r \in R. \end{aligned} \quad (85)$$

Numerical example. In Table 3, solutions of the sPT, sTS1, sTS2, and sTSz models to measure the relative super-efficiencies of DMU_B and DMU_D are summarized to observe how the decision variables are changed. DMU_B and DMU_D have the highest and lowest values on inputs and outputs and computed the super-efficiency scores. The four-phase procedure determines the range of SIC scalars ($\kappa_o^{sTS1}, \kappa_o^{sTS2}$). DMU_B has the lowest value of Y_1 567 and DMU_D has the highest and lowest values of X_2 and Y_2 , 281 and 97. The measured super-efficiencies are comprehensively measured due to the range of SIC scalars, which are predetermined in Phases 1 and 3. ^{xxvi}

^{xxvi} Each of the sPT, sTS1, sTS2, and sTSz models determines τ_o^* in two steps. Those

3.3. The SIC Effects in Measuring the Super-Efficiency

In Figure 5, the coordinates of points O, AP1, AP2, B1, and B2 of the sTS1 and sTS2 models in evaluating DMU_B can be visualized. Eq. (86), Eq. (87), and Eq. (88) compute the slopes of the vectors $\overrightarrow{O, Bc}$, $\overrightarrow{O, APc}$, and $\overrightarrow{APc, Bc}$, respectively, where the choice "c" could be "1" and "2."

$$\bar{m}(\overrightarrow{O, Bc}) = \frac{\beta_o^{c*} - 0}{\alpha_o^{c*} - 0} = \frac{\beta_o^{c*}}{\alpha_o^{c*}}. \quad (86)$$

$$\bar{m}(\overrightarrow{O, APc}) = \frac{\gamma_o \omega_o^{c*} - 0}{-(1 - \gamma_o) \omega_o^{c*} - 0} = \frac{\gamma_o \omega_o^{c*}}{-(1 - \gamma_o) \omega_o^{c*}}. \quad (87)$$

$$\bar{m}(\overrightarrow{APc, Bc}) = \frac{\beta_o^{c*} - \gamma_o \omega_o^{c*}}{\alpha_o^{c*} - [-(1 - \gamma_o) \omega_o^{c*}]} = \frac{u_o^* y_o}{v_o^* x_o}. \quad (88)$$

The same analysis should apply to DMU_D the situation as depicted in Figure 5.

The three vectors have the relationships as shown in Eq. (89). The estimated sTSc super-efficiency score is affected by the SIC.

$$\overrightarrow{O, Bc} = \overrightarrow{O, APc} + \overrightarrow{APc, Bc}; \quad E_o^{sTSc} = \bar{m}(\overrightarrow{O, Bc}) = \frac{\beta_o^{c*}}{\alpha_o^{c*}}. \quad (89)$$

The effects of the SIC within the sTSc model could be visualized as triangular with points O, APc, and Bc in the 2D graphical intuition. The slopes $\bar{m}(\overrightarrow{O, APc})$ and $\bar{m}(\overrightarrow{APc, Bc})$ are not the scale and technical efficiencies.

4. Four-phase b-VGA-EA method

The following presentation is to calibrate (q_o, p_o) to measure the efficiency of DMU_o . It can be applied to measure the super-efficiency. Nonetheless, the PT model estimate (q_o, p_o) may not be achievable DMU_o . The bTSc model with the SIC equates to the choice scalar κ_o^c that identifies the reference peers \mathcal{E}_o^{bTSc} . The benchmarks of inputs and outputs are the function of intensities of the reference peers belonging to \mathcal{E}_o^{bTSc} , as shown in Eq. (33). Section 2.5.4 illustrates the effects of SIC on the solutions.

The four-phase process illustrated in Figure 1 significantly improves the EA of DMUs. This framework is structured around conditions that epitomize a performance improvement problem. It incorporates practical considerations into the PT and bTSc VGA models for systematic solutions.

4.1. Phase-1: PT model Identifies the First SIC Scalar

An initial assessment distinguishes between efficient and inefficient DMUs in the performance evaluation. This distinction is crucial for the subsequent analysis and is primarily based on the existence of a "virtual gap." An inefficient DMU_o is characterized by a positive virtual gap, indicating a discrepancy between its current

VGA models have comprehensive evaluations, but DEA models cannot.

performance and the b-Efficiency Equator. The DMU must undergo a comprehensive four-phase improvement process.

The commencement of this process involves the identification of the first SIC scalar κ_o^1 . This scalar is conceptualized as the sum of the estimated intensities associated with efficient counterparts $\kappa_o^1 = \sum_{\forall j \in \mathcal{E}_o^{PT}} \pi_{jo}^*$. Essentially, it serves as a quantitative measure of the extent to which DMU_o needs to adjust its operations to align with the practices of its reference peers.

Conversely, a DMU identified as efficient exhibits a zero virtual gap, signifying that its performance already aligns with the best practices observed across the dataset at the optimal level. Such DMUs are deemed ineligible for further analysis in Scenario II. For these units, Scenario II presented in Section 3 should be employed for continuous performance management and improvement, ensuring they maintain their efficiency status over time.

4.2. Phase-2: TS1 Model Uses the First SIC Scalar

The comparison between the optimal solutions of the PT and TS1 models in Steps I and II reveals some critical insights. Both models share identical TAP solutions in Step I due to the equality $\tau_o^{PT\#} = \tau_o^{TS1\#}$ and $\sum_{\forall j \in \mathcal{E}_o^{PT}} \pi_{jo}^{\#} = \sum_{\forall j \in \mathcal{E}_o^{TS1}} \pi_{jo}^{\#} = \kappa_o^1$. However, their TVG programs yield two sets of optimal solutions due to the additional v Scalar. This process leads to a specific relationship between their intensities, resulting in disparate benchmarks for performance indices between the two models.

Eq. (90) shows Step I of the PT and TS1 models have the relationships.

$$\begin{aligned} \Delta_o^{TS1\#} = \Delta_o^{PT\#} = \delta_o^{TS1\#} = \Delta_o^{PT\#}; (q_o^{PT\#}, p_o^{PT\#}) &= (q_o^{TS1\#}, p_o^{TS1\#}); \\ (v_o^{PT\#}, u_o^{PT\#}) \neq (v_o^{TS1\#}, u_o^{TS1\#}); \sum_{\forall j \in \mathcal{E}_o^{PT}} \pi_{jo}^{\#} &= \sum_{\forall j \in \mathcal{E}_o^{TS1}} \pi_{jo}^{\#} = \kappa_o^1. \end{aligned} \quad (90)$$

Note the best peers' intensities, $\pi_{jo}^{PT\#}$, and $\pi_{jo}^{TS1\#}$, may be different; therefore, the benchmarks of performance indices of the two models are distant. They have identical solutions on the dual variables. But have different primal solutions.

Step II further differentiates the two models. Although their TAP programs provide the same total values, their goal prices and other variables differ. This disparity leads to different efficiency measurements: $E_o^{PT\star}$ represents pure technical efficiency, and $E_o^{TS1\star}$ comprises the effects on the *gray virtual input and output* and scalar prices. Notably, the SIC scalar is a crucial factor in evaluating DMU_o . In Step II of PT and TS1 models, the TAP programs equal to $(\sum_{\forall i \in I} q_{io}^* + \sum_{\forall r \in R} p_{ro}^*)$ multiplies the distinct virtual goal prices $\tau_o^{PT\star}$ $\tau_o^{TS1\star}$. The PT and TS1 models have the relationships shown in Eq. (91).

$$\begin{aligned} \tau_o^{TS1\star} \neq \tau_o^{PT\star}, \Delta_o^{TS1\star} \neq \Delta_o^{PT\star}; (v_o^{PT\star}, u_o^{PT\star}) &\neq (v_o^{TS1\star}, u_o^{TS1\star}); \\ (q_o^{PT\star}, p_o^{PT\star}) = (q_o^{TS1\star}, p_o^{TS1\star}); 0 < E_o^{PT\star} \neq E_o^{TS1\star} &\leq 1. \end{aligned} \quad (91)$$

4.3. Phase-3: Identifying the Second SIC Scalar

The standard sensitivity analysis of the LP TS1 model involves perturbing the κ_o^1 scalar, which results in allowable decreases and increases. Specifically, κ_o^2 equals κ_o^1 minus the allowable decrease or κ_o^2 equals κ_o^1 plus the allowable increase, as expressed in Eq. (92).

$$\begin{aligned} \kappa_o^2 &= \kappa_o^1 - (\text{allowable decreasing of } \kappa_o^1), \\ \text{or } \kappa_o^2 &= \kappa_o^1 + (\text{allowable increasing of } \kappa_o^1). \end{aligned} \quad (92)$$

The final SIC scalar κ_o^c in Phase-4 is linked to κ_o^1 in Phase-1. These bounds (κ_o^1 and κ_o^2) represent the possible range of SIC scalars (κ_o^c) within the bTSc model. If $w_o^{TS1^*}$ and $w_o^{TS2^*}$ are more significant than 0, $\kappa_o^1 < \kappa_o^c < \kappa_o^2$. Otherwise, $\kappa_o^1 > \kappa_o^c > \kappa_o^2$.

The best peers in the TS1 and TS2 models remain consistent, as indicated by $\mathcal{E}_o^{TS1} = \mathcal{E}_o^{TS2} = \mathcal{E}_o^{bTSc}$. However, the estimated intensities of these peers differ $\pi_o^{TS1^*} \neq \pi_o^{TS2^*}$. The solutions of these models exhibit relationships detailed in Eq. (93), displaying discrepancies in the estimated variables, such as:

$$\begin{aligned} \tau_o^{TS1^*} &\neq \tau_o^{TS2^*}; & (v_o^{TS1^*}, u_o^{TS1^*}) &\neq (v_o^{TS2^*}, u_o^{TS2^*}); \\ w_o^{TS1^*} &\neq w_o^{TS2^*}; & (q_o^{TS1^*}, p_o^{TS1^*}) &\neq (q_o^{TS2^*}, p_o^{TS2^*}). \end{aligned} \quad (93)$$

4.4. Phase-4: Select the Final Scalar Within the Region

Phases -1, -2, and -3 integration confirms DMU_o 's learning process with the reference peers, whose total intensities are bounded within the κ_o^1 and κ_o^2 . Phase-4, a critical decision-making step, involves selecting the final scalar κ_o^z for the bTSz model. DMU_o undertakes several trials in choosing scalars in Phase-4 to determine a preferred final scalar κ_o^z . Each choice scalar corresponds to a unique set of estimated intensities and benchmarks of inputs and outputs \hat{x}_{io}^{bTSz} and \hat{y}_{ro}^{bTSz} derived from efficient peers.

By emulating the reference peers based on the estimated intensities, DMU_o gains insights into feasible and desirable productivity benchmarks. This interactive approach ensures a more thorough evaluation DMU_o . Exploring different SIC scalars and model variations aids in comprehending the diverse impacts these factors have on assessments. Ultimately, this process helps make better-informed management decisions regarding productivity and efficiency.

DMU-o may redefine the datasets by altering the performance indices and DMUs and repeating the four-phase procedure.

5. Numerical examples and the 2D geometric intuitions

The numerical example depicted in Table 1. Table 2 summarizes the efficiency measurements of DMU_K , DMU_o , within Scenario-I by the PT, TS1, TS2, and TS3 models. The PT model evaluated DMU_B and DMU_D and confirmed they

are efficient units. Section 5.2 offers Scenario II to measure the super-efficiencies of efficient DMUs.

5.1. Measures the Inefficiencies

5.1.1. Relationships Between PT and TS1 Models in Step I

Eq. (18) and Eq. (35) are used to calculate the total adjustment prices ($\Delta_o^{PT\#} = \delta_o^{TS1\#}$) and total virtual gaps ($\Delta_o^{PT\#} = \Delta_o^{TS1\#}$), using specific data provided in row R2 of Table 2. Each amount is \$2.3010. Additionally, the TS1-I model incorporates the SIC impact through the *vScalar*, $\omega_o^{1\#}$ ($=\$2.479$), in calculating the total virtual gap. This result demonstrates how the virtual gap, considering the SIC and *vScalar* in the TS1-I model, maintains the same value as in the PT-I model, indicating a consistent evaluation despite including additional factors.

5.1.2. Compare the PT and TS3 Models

By try and error, we identified κ_o^3 equals 0.718 to have $E_o^{PT^*} = E_o^{TS3^*}$ ($=0.589$). The columns of PT-II and TS3-II in Table 2 list the estimated solutions, in which rows R8 and R9 are the two virtual technology sets, (α_j^*, β_j^*) and $(\alpha_j^{3*}, \beta_j^{3*})$, where $DMU_j = (A, B, D, G, H, K)$, as per Eq. (12), Eq. (28), and Eq. (29).

Via Eq. (43) and Eq. (44), the locations of Tp, $(\hat{\alpha}_o^*, \hat{\beta}_o^*)$ and point T3, $(\hat{\alpha}_o^{3*}, \hat{\beta}_o^{3*})$ on the b-Efficiency Equator are obtained. The estimated rectilinear distances from points Kp to Tp and from point K3 to T3 are $\Delta_o^{PT^*}$, and $\delta_o^{TS3^*}$, see the expressions in the upper-left corner of Figure 3. Section 2.5.4 illustrated the SIC affected the estimations as shown in Eq. (52).

In Figure 3, each point signifies a DMU_j within the virtual technology sets of the PT-II ($\Phi_o^{PT^*}$) and TS3-II models ($\Phi_o^{TS3^*}$), respectively. The points (Ap, Bp, Dp, Gp, Hp, Kp) and (A3, B3, D3, G3, H3, K3) are located at (α_j^*, β_j^*) and $(\alpha_j^{3*}, \beta_j^{3*})$. The blue dashed lines graphically represent the vectors $\overrightarrow{O, K3} \overrightarrow{AP3}, \overrightarrow{K3}$. The red dashed line indicates the vector $\overrightarrow{O, Kp}$ of pure technical efficiency, $E_o^{PT^*} = \beta_o^{3*} / \alpha_o^{3*}$. Inefficient DMUs are situated under the b-Efficiency Equator.

5.1.3. Compare the Solutions between TS1 and TS2 models

Figure 4, similar to Figure 3, depicts the locations of DMUs in the TS1-II and TS2-II models, respectively, (A1, B1, D1, G1, H1, K1) and (A2, B2, D2, G2, H2, K2). Their coordinates, $(\alpha_j^{1*}, \beta_j^{1*})$ and $(\alpha_j^{2*}, \beta_j^{2*})$, are listed in rows R8 and R9. DMUs B and D emerge as efficient peers with their intensities π_{oB}^* and π_{oD}^* . R4 detailed the benchmarks of inputs and outputs. R5 lists the virtual prices. R6 contains the benchmark virtual scales. R7 lists $\Xi_o^{bTSc^*}$ and $E_o^{bTSc^*}$. Since $w_o^* > 0$, decreasing κ_o^1 ($=1.5153$) to κ_o^2 ($=0.515$), DMU_o exhibits decreasing RTvS: $\Xi_o^{TS1^*}$ ($= 2.435$) $>$ $\Xi_o^{TS2^*}$ ($= 1.497$).

At the same time, the relative efficiency is increasing, $E_o^{TS1^*}$ ($=0.411$) less than

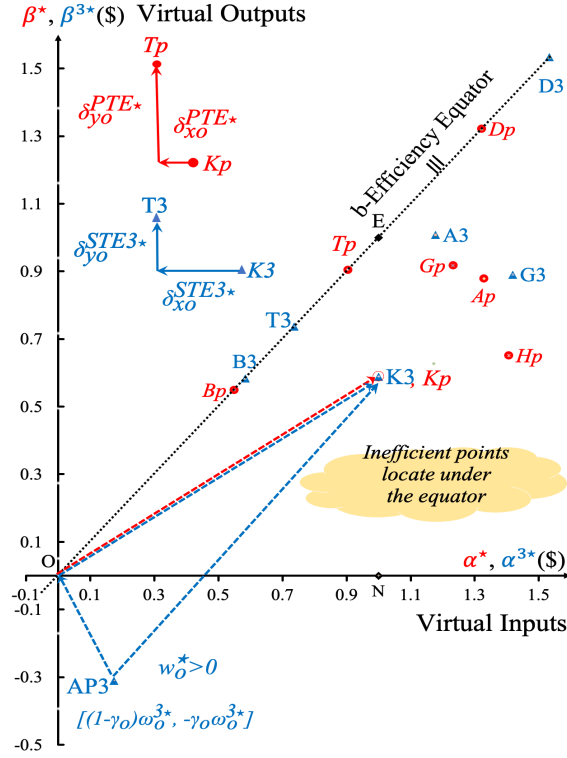


Fig. 3. Comparing the solutions of PT and TS3 models.

E_o^{TS2*} (=0.688). However, DMU_o may use Eq. (48) to analyze the interlinkage relationships between input and output indices for managing the performance indices.

The bTSc program introduces an *anchor point* (APc) located at the point $[(1 - \gamma_o)\kappa_o^c w_o^*, -\gamma_o \kappa_o^c w_o^*]$ denotes as $[AP(x), AP(y)]$. Anchor points are located in the second and fourth quadrants when $w_o^* > 0$ and $w_o^* < 0$. The rectilinear distance between point APc and the origin O is the vScalar, $\kappa_o^c w_o^*$. In Figure 4, the anchor points of the TS1 and TS2 models are located at AP1 and AP2. Because $w_o^* > 0$, the two anchor points are located in the fourth quadrant. The TS3 model interpolates TS1 and TS2 models, providing a framework for determining the optimal scalars κ_o^3 within the interval of SIC scalars. Using the scalar κ_o^3 between κ_o^1 and κ_o^2 , the TS3 model has the anchor points, and AP3 is located between AP1 and AP2.

DMU_j lies in the fourth quadrant if, according to Eq. (2), one could have $\Delta_j^{bTSc*} > \$0$. ($\alpha_j^{c*} > \$0, \beta_j^{c*} < \0), and their ratio is less than zero. Conversely, DMU_j is in the third quadrant if ($\alpha_j^{c*} < \$0, \beta_j^{c*} < \0), and their ratio is more significant than zero.

Section 2.5.4 illustrated the SIC affected the estimations as shown in Eq. (53).

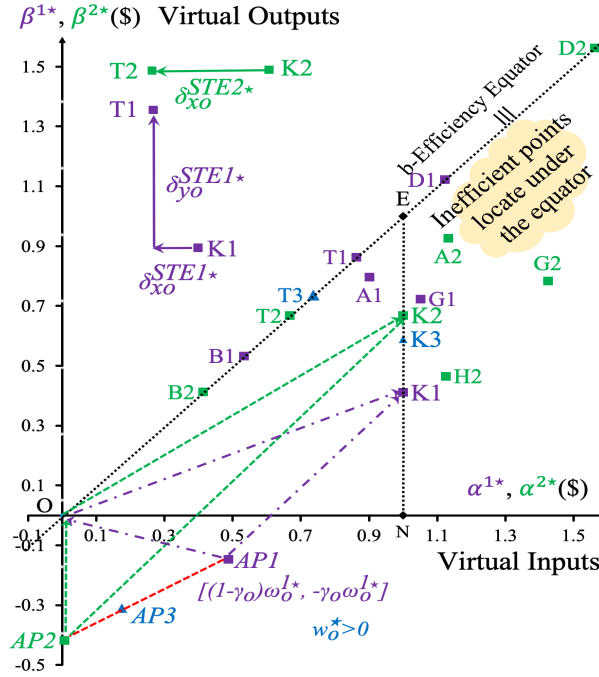


Fig. 4. Comparing the solutions of TS1 and TS2 models.

Therefore, eliminating an inefficient DMU_j from (X, Y) does not impact the evaluation. We can visually interpret the effects under the SIC scalars κ_o^1 and κ_o^2 using geometric vectors. In Figure 4, the purple color dashed lines express the three vectors $\overrightarrow{O, K1}$, $\overrightarrow{AP1, O}$, and $\overrightarrow{AP1, K1}$ of the TS1 model can be found.

Similarly, the green color dashed lines express the three vectors $\overrightarrow{O, K2}$, $\overrightarrow{AP2, O}$, and $\overrightarrow{AP2, K2}$ of the TS2 model. The three vectors $\overrightarrow{O, K3}$, $\overrightarrow{AP3, O}$, $\overrightarrow{AP3, K3}$ of the TS3 model are not depicted. Point $K3$ is located between points $K1$ and $K2$ on the normalization vertical line (N, E) . Using the final SIC scalar κ_o^z in the $bTSSz$ model, points APz , Kz , and Tz are located between points $(AP1$ and $AP2)$, $(K1$ and $K2)$, and $(T1$ and $T2)$, respectively. The three vectors, $\overrightarrow{O, Kz}$, $\overrightarrow{APz, O}$, $\overrightarrow{APz, Kz}$, shall be visualized in Figure 4, similar to Eq. (53). The upper left corner of the figure depicts the rectilinear distances of DMU_o the project on the b-Efficiency Equator.

5.2. Measures the Super-efficiencies

Scenario-I confirmed DMU_B and DMU_D are efficient. Scenario II employs the sPT and sTSc models to measure their super-efficiencies in the four-phase procedure. Table 3 summarizes the solutions of the sPT, sTS1, sTS2, and sTSz models. For simplicity, in rows R8 and R9, the values of α_{oK}^* , β_{oK}^* , α_{oH}^* , and β_{oH}^* are not shown.

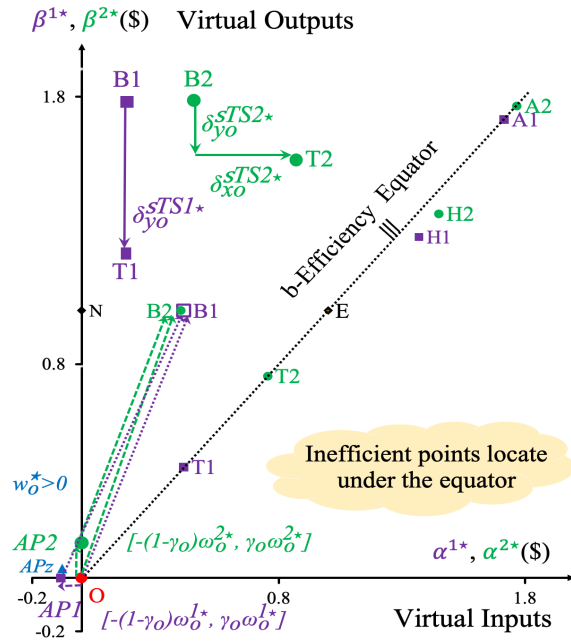


Fig. 5. Comparing the solutions of sTS1 and sTS2 models in assessing DMU_B .

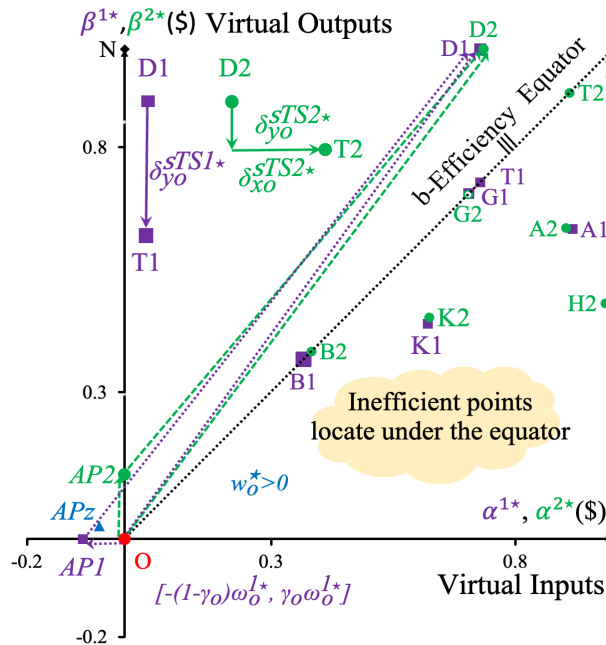


Fig. 6. Comparing the solutions of sTS1 and sTS2 models in assessing DMU_D .

Table 2. Evaluate Inefficiencies for DMU_K , DMU_B , and DMU_D by Scenario-I.

Row	Sol.	$DMU_o=$ Unit	K		K		K		K		B		D	
			PT-I Phase-1	PT-II	TS1-I Phase-2	TS1-II	TS2-I Phase-3	TS2-II	TS3-II Ph.-4	PT-II Ph.-1	PT-II Ph.-1			
R1	κ_o^c	-	1.5153	1.5153	1.5153	1.5153	0.5150	0.5150	0.718	1	1			
	τ_o	\$	1	0.179	1.000	0.256	1.000	0.500	0.413	0.500	0.266			
R2	Δ_o, δ_o	\$	2.3010	0.4113	2.3010	0.5893	0.6643	0.3321	0.411	0	0			
	v_{1o}	\$/ton	2.8713	0.5133	0.6250	0.1601	0.6250	0.3125	0.258	0.500	0.387			
	v_{2o}	\$/hr	0.0069	0.0012	0.0069	0.0018	0.0069	0.0034	0.003	0.017	0.001			
	u_{1o}	\$/m ³	0.0022	0.0004	0.0011	0.0003	0.0011	0.0006	0.0005	0.001	0.0003			
	u_{2o}	\$ / %	0.0204	0.0036	0.0204	0.0052	0.0204	0.0102	0.008	0.006	0.003			
	w_o	\$	0	0	1.6362	0.4190	1.6362	0.8181	0.675	0	0			
R3	q_{1o}	-	0	0	0	0	0.4554	0.4554	0.363	0	0			
	q_{2o}	-	0.5334	0.5334	0.5334	0.5334	0.2089	0.2089	0.275	0	0			
	p_{1o}	-	0	0	0	0	0	0	0	0	0			
	p_{2o}	-	1.7677	1.7677	1.7677	1.7677	0	0	0.359	0	0			
	π_{oB}	-	1.421	1.421	1.421	1.421	0.119	0.119	0.383	1	0			
	π_{oD}	-	0.094	0.094	0.094	0.094	0.396	0.396	0.335	0	1			
R4	\hat{x}_{1o}	ton	1.6	1.6	1.6	1.6	0.8713	0.8713	1.019	1.0	1.9			
	\hat{x}_{2o}	hr	67.66	67.66	67.66	67.66	114.72	114.72	105.165	29	281			
	\hat{y}_{1o}	m ³	1036	1036	1036	1036	1036	1036	1036	567	2446			
	\hat{y}_{2o}	%	135.6	135.6	135.6	135.6	49.0	49.0	66.58	89	97			
	γ_o	-	0.232	0.232	0.232	0.232	1.000	1.000	0.640	0	0			
	ω_o^c	\$	0	0	2.479	0.635	0.843	0.421	0.485	0	0			
R5	$x_{1o}v_{1o}$	\$	4.594	0.821	1.000	0.256	1.578	0.789	0.689	0.500	0.734			
	$x_{2o}v_{2o}$	\$	1.000	0.179	3.479	0.891	1.265	0.632	0.622	0.500	0.266			
	$y_{1o}u_{1o}$	\$	2.293	0.410	1.178	0.302	1.178	0.589	0.486	0.500	0.734			
	$y_{1o}u_{1o}$	\$	1.000	0.179	3.479	0.891	1.843	0.921	0.898	0.500	0.266			
R6	α_o, α_o^c	\$	5.594	1.000	3.905	1.000	2.000	1.000	1.000	1	1			
	β_o, β_o^c	\$	3.293	0.589	1.604	0.411	1.336	0.668	0.589	1	1			
	$\hat{\alpha}_o, \hat{\alpha}_o^c$	\$	5.061	0.905	3.371	0.863	1.336	0.668	0.737	1	1			
	$\hat{\beta}_o, \hat{\beta}_o^c$	\$	5.061	0.905	3.371	0.863	1.336	0.668	0.737	1	1			
R7	Ξ_o	-	1.699	1.699	2.435	2.435	1.497	1.497	1.699	1	1			
	E_o	-	0.589	0.589	0.411	0.411	0.668	0.668	0.589	1	1			
R8	α_A, α_A^c	\$	7.432	1.000	3.522	0.902	2.265	1.133	0.902	3.219	1.002			
	α_B, α_B^c	\$	3.071	1.328	2.082	0.533	0.825	0.413	0.533	1	0.414			
	α_D, α_D^c	\$	7.393	0.549	4.382	1.122	3.125	1.563	1.122	5.795	1			
R9	β_A, β_A^c	\$	4.917	0.879	3.110	0.796	1.853	0.926	0.796	1.715	0.664			
	β_B, β_B^c	\$	3.071	0.549	2.082	0.533	0.825	0.413	0.533	1	0.414			
	β_D, β_D^c	\$	7.393	1.322	4.382	1.122	3.125	1.563	1.122	2.702	1			
R10	AP(x)	\$	-	-	1.905	0.488	0	0	0.175	-	-			
	AP(y)	\$	-	-	-0.575	-0.147	-0.843	-0.421	-0.310	-	-			

Table 3. Solutions in Measuring the Super-Efficiencies of DMU_B and DMU_D by Scenario-II.

Row	Sol.	Unit	$DMU_o =$							
			B	B	B	B	D	D	D	D
			sPT-II Ph.-1	sTS1-II Ph.-2	sTSz-II Ph.-4	sTS2-II Ph.-3	sPT-II Ph.-1	sTS1-II Ph.-2	sTSz-II Ph.-4	sTS2-II Ph.-3
R1	κ_o^c	-	0.2417	0.2417	0.3345	0.4273	1.3411	1.3411	1.4092	1.4774
	τ_o	\$	0.5	0.5	0.4823	0.4591	0.7709	0.8037	0.7827	0.7614
	Δ_o, δ_o	\$	0.5855	0.5855	0.5964	0.5979	0.2611	0.2722	0.2688	0.2652
R2	v_{1o}	\$/ton	0	0	0	0	0.3889	0.4230	0.4119	0.4007
	v_{2o}	\$/hr	0.0143	0.0172	0.0166	0.0158	0	0	0	0
	u_{1o}	\$/ m^3	0.0009	0.0009	0.0009	0.0008	0.0003	0.0003	0.0003	0.0003
	u_{2o}	\$/%	0.0056	0.0056	0.0054	0.0052	0.0024	0.0020	0.0020	0.0019
	w_o	\$	0.0000	0.3538	0.3413	0.3249	0	0.0566	0.0551	0.0536
R3	q_{1o}	-	0	0	0	0	0.0000	0.1156	0.2313	
	q_{2o}	-	0	0	0.3840	0.7681	0	0	0	0
	p_{1o}	-	0.4344	0.4344	0.2172	0.0000	0.3387	0.3387	0.2278	0.1170
	p_{2o}	-	0.7366	0.7366	0.6355	0.5343	0	0	0	0
	π_{oA}	-	0.2417	0.2417	0.3345	0.4273	0	0	0	0
	π_{oB}	-	0	0	0	0	0.6424	0.6424	0.5211	0.3997
	π_{oG}	-	0	0	0	0	0.6986	0.6986	0.8881	1.0776
R4	\hat{x}_{1o}	ton	1	1	1	51.273	1.9	1.9	2.119	2.339
	\hat{x}_{2o}	hr	29	29	40.137	567	281	281	281	281
	\hat{y}_{1o}	m^3	320.7	320.7	443.8	41.4	1617.6	1617.6	1888.8	2159.9
	\hat{y}_{2o}	%	23.442	23.442	32.444	0.5897	97	97	97	97
	γ_o	-	0	0	0.3105	0.1388	0	0.0000	0.3367	0.6642
	ω_o^c	\$	0	0.0855	0.1142	0	0	0.0759	0.0776	0.0792
	R5	$x_{1o}v_{1o}$	\$	0	0	0	0.4591	0.7389	0.8037	0.7827
$x_{2o}v_{2o}$		\$	0.4145	0.5	0.4823	0.4591	0	0	0	0
$y_{1o}u_{1o}$		\$	0.5	0.5	0.4823	0.4591	0.7709	0.8037	0.7827	0.7614
$y_{2o}u_{2o}$		\$	0.5	0.5	0.4823	0.4021	0.2291	0.1963	0.1912	0.1860
R6	$\hat{\alpha}_o, \hat{\alpha}_o^c$	\$	0.4145	0.4145	0.5888	0.7547	0.7389	0.7278	0.8217	0.9109
	$\hat{\beta}_o, \hat{\beta}_o^c$	\$	0.4145	0.4145	0.5888	0.7547	0.7389	0.7278	0.8217	0.9109
R7	Ξ_o	-	0.4145	0.4145	0.4036	2.4868	0.7389	0.7278	0.7312	0.7348
	E_o	-	2.4126	2.4126	2.4779	2.1621	1.3533	1.3740	1.3676	1.3609
R8	$\alpha_{oA}, \alpha_{oA}^c$	\$	1.7151	1.7151	1.7603	1.7663	0.8945	0.9163	0.9109	0.9037
	$\alpha_{oB}, \alpha_{oB}^c$	\$	0.4145	0.4145	0.4036	0.4021	0.3889	0.3664	0.3754	0.3827
	$\alpha_{oD}, \alpha_{oD}^c$	\$	4.0163	4.4910	4.4378	3.8242	0.7389	0.7278	0.7312	0.7348
	$\alpha_{oG}, \alpha_{oG}^c$	\$	3.5732	3.9565	3.9222	1.4497	0.7000	0.7048	0.7049	0.7033
R9	β_{oA}, β_{oA}^c	\$	1.7151	1.7151	1.7603	1.7663	0.6473	0.6323	0.6343	0.6347
	β_{oB}, β_{oB}^c	\$	1	1	1	1	0.3889	0.3664	0.3754	0.3827
	β_{oD}, β_{oD}^c	\$	2.702	2.702	2.712	1.938	1	1	1	1
	β_{oG}, β_{oG}^c	\$	1.902	1.902	1.941	1.362	0.7000	0.7048	0.7049	0.7033
R10	AP(x)	\$	0	-0.0855	-0.0787	0.0000	0	-0.076	-0.051	-0.027
	AP(y)	\$	0	0	0.0354	0.1313	0	0	0.026	0.053

To illustrate the fourth phase, we assume the final SIC scalars are the mid-point of the interval of κ_o^1 and κ_o^2 . The anchor point of the sTSz model that contains the SIC scalar κ_o^z , APz is located in the region of points O, AP1, and AP2 because DMU_o is excluded from Eq. (59). In Figure 5, AP1 and AP2 are in the second quadrant because $\omega_o^c > \$0$. When $\omega_o^c > \$0$, the anchor point will be located in the fourth quadrant. R6 in Table 3 listed the locations of DMU_o and its projection points on the b-b-Efficiency Equator. DMU_o is located in the first quadrant and above the b-Efficiency Equator. DMU_o projects on the b-Efficiency Equator, the T1 and T2 in Figures 5 and 6. The reference peers of DMU_B , A1, and A2 are on the b-Efficiency Equator, while the remaining inefficient DMUs lie under it. In evaluating DMU_D , DMU_B , and DMU_G , they are located on the b-Efficiency Equator.

In Table 3, DMU_B has higher super-efficiencies (see R7), which reduced the outputs will have an efficiency score equal to 1. Regarding EA, DMU_B has strong outputs and can be selected as the best alternative to the MCDM problem.

6. Discussions

Our EA method effectively estimates the necessary and achievable adjustments for inputs and outputs. Since the b-VGA-EA method is iterative, it can be refined over time as new data is incorporated or the operational context of the DMUs evolves. Our MCDM method assists decision-makers in efficiently selecting the best DMU, contributing significantly to the decision-making community.

The VGA models systematically measured the unified goal price, τ_o^* of inputs and outputs DMU_o in two steps to ensure the objective virtual gap within the range of ($\$0, \1) so that the dimensionless relative efficiencies and relative super-efficiency could be obtained precisely.

The current b-VGA-EA method could be modified to the w-VGA-EA method to evaluate each DMU in the light of worst practice. In this context, Scenario I and Scenario II are redefined as Scenario III and Scenario IV, respectively.

The PT, bTSc, sPT, and sTSc models are modified to wPT, wTSc, hPT, and hTSc models. The wPT and wTSc models estimate the worst-relative efficiency of DMU_o , where $E_o^* > 1$. By adjusting the input and output ratios, the worst-relative efficiency will deteriorate from $E_o^* > 1$ to $E_o^* = 1$.

The hPT and hTSc models estimate the hypo-relative efficiency of DMU_o , where $E_o^* < 1$. Here, adjusting the input and output ratios improves the hypo-relative efficiency from $E_o^* < 1$ to $E_o^* = 1$. In a similar fashion to the b-VGA-MCDM method, the w-VGA-MCDM method can be used to select the worst DMU through a process involving three analogous stages.

The pair of b-VGA-EA and w-VGA-EA methods are both necessary and essential for assessing each DMU. We plan to publish the w-VGA-EA method alongside the w-VGA-MCDM method to provide comprehensive evaluations.

In practical decision-making, it may be necessary to restrict the adjustment ratios. The b-VGA-EA and w-VGA-EA methods can be extended to create several

r-VGA-EA methods. For example, by omitting $\sum_{\forall i \in I} q_{io} \tau_o$ and $\sum_{\forall r \in R} p_{ro} \tau_o$ in the objective functions of the eight b-VGA and w-VGA models, one can obtain output-oriented and input-oriented measurements. In non-stationary scenarios, where X_a and Y_b are restricted from being adjusted, the objective functions of the eight VGA models can be modified to: $\delta_o^{TAP*} = \min \sum_{\forall i \in I \neq a} q_{io} \tau_o + \sum_{\forall r \in R \neq b} p_{ro} \tau_o$.

Typically, the adjustment ratios of inputs (q_o) range between 0 and 1, while outputs (p_o) may exceed 1. The specific requirement is possible to be met by imposing constraints such as ($p_o \leq 1$) or define upper and lower bounds: $\underline{q}_o \leq q_o \leq \bar{q}_o$ and $\underline{p}_o \leq p_o \leq \bar{p}_o$. The r-VGA-MCDM methods could be generated to meet the practical conditions.

The practical issues addressed in the DEA literature¹⁰, such as the Malmquist Index, network DEA, free-disposal hull, input/output sharing, and input/output selection, can be considered solvable using VGA models. These models can also be adapted to handle datasets containing zeros and negatives¹¹. Additionally, VGA models are helpful for datasets with bounded data, ordinal data, and ratio-bounded data³².

Further research could explore the development of integrated models that combine the strengths of both MCDM and EA, tailored to specific sectors such as healthcare, energy, and public services. Methodological advancements in addressing uncertainty, adapting to dynamic conditions, and incorporating sustainability dimensions are promising avenues to enhance the applicability and impact of these decision-support tools. In conclusion, the synergy between MCDM methods and EA offers significant potential for advancing sophisticated and practical decision-making frameworks, ultimately improving system performance and supporting the achievement of strategic goals across various contexts.

The TAP program of a VGA model uses a standard form of linear programming with $(n + m + s)$ columns and $(m + s + 1)$ rows. This problem can be solved efficiently with free linear programming software on a notebook computer. A software procedure can be created to execute the EA and MCDM methods, ensuring quick execution, including the preparation of EA and MCDM reports and 2D graphical visualizations.

Acknowledgment

We thank the referees for their valuable comments. This research received no specific grant from public, commercial, or not-for-profit funding agencies. We have no competing interests to declare. We confirm that the data supporting the findings of this study are available within the article.

References

1. S. K. Sahoo and S. S. Goswami, A Comprehensive Review of Multiple Conditions Decision-Making (MCDM) Methods: Advancements, Applications, and Future Directions. *Decision Making Advances*, 1(1)(2023) 25–48.

2. S. B. Amor, F. Belaid, R. Benkraiem, B. Ramdani, and K. Guesmi, Multi-criteria classification, sorting, and clustering: a bibliometric review and research agenda. *Ann. Oper. Res.*, **325**(2)(2022) 1-23, doi:10.1007/s10479-022-04986-9.
3. A. Charnes, W. W. Cooper and E. Rhodes, Measuring the Efficiency of Decision-Making Units, *Eur. J. Oper. Res.* **2** (7)(1978) 429–44.
4. W. W. Cooper, L. M. Seiford and K. Tone, *Data Envelopment Analysis: A Comprehensive Text with Models, Applications, References, and DEA-Solver Software* 2nd ed. (Springer-Verlag, New York, 2007).
5. G. B. Dantzig and M. N. Thapa, *Linear Programming 1: Introduction* (Springer-Verlag, 1997).
6. A. Emrouznejad and G.-L. Yang, A survey and analysis of the first 40 years of scholarly literature in DEA: 1978–2016. *Socio-Econ. Plan. Sci.* **61**(2018) 4–8.
7. R. C. Sickles and V. Zelenyuk, *Measurement of Productivity and Efficiency: Theory and Practice*, (Cambridge University Press, 2019), doi:10.1017/9781139565981.
8. M. Halická and M. Trnovská, A unified approach to non-radial graph models in data envelopment analysis: common features, geometry, and duality. *Eur. J. Oper. Res.* **289**(2)(2021) 611–627, doi:10.1016/j.ejor.2020.07.019.
9. R. G. Dyson, R. Allen, A. S. Camanho, V. V. Podinovski, C. S. Sarrico and E. A. Shale, Pitfalls and protocols in DEA. *Eur. J. Oper. Res.* **132**(2)(2001)245–259.
10. A. Panwar, M. Olfati, M. Pant, and V. Snasel, A Review on the 40 Years of Existence of Data Envelopment Analysis Models: Historic Development and Current Trends. *Arch. Comput. Methods Eng.* **29**(7)(2022) 5397–5426.
11. T. Sueyoshi and M. Goto, Pitfalls and Remedies in DEA Applications: How to Handle an Occurrence of Zero in Multipliers by Strong Complementary Slackness Conditions. *Engineering* **5**(5)(2013) 29–34.
12. A. Mergoni and K. D. Witte, Policy evaluation and efficiency: a systematic literature review. *Int. Trans. Oper. Res.* **29**(3)(2021) 1337-1359.
13. M. Zarrin, J. Schoenfelder and J. O. Brunner, Homogeneity and Best Practice Analyses in Hospital Performance Management: An Analytical Framework. *Health Care Manag. Sci.* **25**(3)(2022) 406–425.
14. R. Brown, Mismanagement or mismeasurement? Pitfalls and protocols for DEA studies in the financial services sector. *Eur. J. Oper. Res.* **174**(2)(2006) 1100-1116.
15. S. Kumbhakar and C.A.K. Lovel, *Stochastic Frontier Analysis*, (Cambridge University Press, 2000).
16. M. Madaleno and V. Moutinho, Stochastic Frontier Analysis: A Review and Synthesis, in *Advanced Mathematical Methods for Economic Efficiency Analysis*, eds. P. Macedo, V. Moutinho, and M. Madaleno, Lecture Notes in Economics and Mathematical Systems, (Springer, Cham. 2023) pp.55-78.
17. Y. C. Hwang, *Virtual-gap measurement for assessing a set of units*, (in Chinese) Advisor F. F.-H. Liu (Unpublished master thesis, National Yang Ming Chiao Tung University, Taiwan 2014).
18. F. F.-H. Liu and Y. C. Liu, Procedure to Solve Network DEA Based on a Virtual Gap Measurement Model. *Math. Probl. Eng.* **2017**(2017a) 1-13.
19. F. F.-H. Liu and Y. C. Liu, A methodology to assess the supply chain performance based on gap-based measures. *Comput. Ind. Eng.* **110**(2017b) 550-559.
20. Z.-Y. Lin, *Analysis of product mix strategy for camping supplies stores*, (in Chinese) Advisor S.-C. Shih (Unpublished masters thesis, Providence University, Taiwan 2024).
21. J.-C. Li, *Evaluating the internet word-of-mouth performance of the hotel industry through online travel reviews*, (in Chinese) Advisor S.-C. Shih (Unpublished masters thesis, Providence University, Taiwan 2022).

22. F. Aleskerov and V. Petrushchenko, DEA by sequential exclusion of alternatives in heterogeneous samples. *IJITDM*. **15**(1)(2016) 5-22.
23. W. W. Zhu, Y. Yu and P. P. Sun, Data envelopment analysis cross-like efficiency model for non-homogeneous decision-making units: The case of United States companies' low-carbon investment to attain corporate sustainability. *Eur. J. Oper. Res.* **269**(1)(2018) 99–110.
24. W. H. Li, L. Liang, W. D. Cook, and L. Zhu, DEA models for non-homogeneous DMUs with different input configurations. *Eur. J. Oper. Res.* **254**(3)(2016) 946-956.
25. K. Tone, A slack-based measure of efficiency in data envelopment analysis. *Eur. J. Oper. Res.* **130**(2001), 498–509.
26. K. Tone, A slacks-based measure of super-efficiency in data envelopment analysis. *Eur. J. Oper. Res.* **143**(2002), 32–41.
27. R. D. Banker, A. Charnes and W. W. Cooper, Some Models for Estimating Technical and Scale Inefficiencies in Data Envelopment Analysis. *Manage Sci.* **30**(9)(1984) 1078–92.
28. V.V. Podinovski, F. R. Førsund, Scale Elasticity and Returns to Scale, in *Handbook of Production Economics*, eds. S. C. Ray, R. G. Chambers, S. C. Kumbhakar, (Springer, Singapore 2022) 682-718, doi.org/10.1007/978-981-10-3455-8-23.
29. R. D. Banker, W. W. Cooper, L. M. Seiford, R. M. Thrall and J. Zhu, Returns to scale in different DEA models. *Eur. J. Oper. Res.* **154**(2004) 345–362.
30. P. Liu, H. Xu, and K. Xu, A new DEA model for slacks-based measure of efficiency and super-efficiency with strongly efficient projections. *Intl. Trans. in Op. Res.* **32**(2025) 1033-1063, doi.org/10.1111/itor.13342.
31. Y. Chen, Y. Li and L. Liang and H. Wu, An extension on super slacks-based measure DEA approach. *Ann. Oper. Res.*, **278**(1)(2019), 101-121, doi:10.1007/s10479-017-2495-2.
32. J. Zhu, Imprecise data envelopment analysis (IDEA): A review and improvement with an application. *Eur. J. Oper. Res.* **144**(3)(2003) 513-529, doi.org/10.1016/S0377-2217(01)00392-7.